Università degli Studi di Padova

Facoltà di: **Ingegneria**

Corso di Laurea in: **Bioingegneria**

Modeling the effect of oscillation in receptor expression on synchrony in the mammalian circadian model

Laureanda: Claudia Saccoman

Relatore: Chiar.ma Prof.ssa Barbara Di Camillo

Correlatori:

Chiar.mo Prof. Francis J. Doyle III

Chiar.mo Dott. Bharath Ananthasubramaniam

Anno Accademico 2010/2011

Ai Miei Genitori

Abstract

The Mammalian Circadian System is the fundamental intracellular mechanism responsible for timekeeping, giving to life a notion of biological time. The suprachiasmatic nucleus (SCN) is located in the hypothalamus and contains the circadian mammalian pacemaker that is responsible for endogeneous biological timekeeping. It is a network of neurons, each is a limit-cycle oscillator, characterized by a standard waveform and period to which they return every time after a perturbation occurs. In each single neuron transcriptional activators and repressors bind target sequences in the promoter regions of the genes, generating the rhythmicity in interlocked feedback loops of activations and repressions of clock-gene transcriptions. Two main families of genes are involved: period (*Per1, Per2, Per3*) and Cryptocrome (*Cry1, Cry2*) which transcriptions are activated by heteromeric complexes containing CLOCK and BMAL1 proteins. *Per* and *Cry* mRNA levels accumulate. *Per* and *Cry* proteins expression is delayed by several hours and peaks in the nuclei repressing their gene transcription in a negative feedback loop. CRY proteins form repressor complexes that physically associate with *Bmal1/Clock* complex, inhibiting their activity thus inhibit the transcription. Gradual loss of PER and CRY proteins leads to de-repression, and then the daily cycle starts anew (Herzog 2007, Hastings et al. 2007, 2008, Weber 2009, Ukai-Tadenuma et al. 2011). The SCN is made of multiple clocks that communicate to synchronize and oscillate on phase at a steady-state.

The neurotransmitter Vasoactive Intestinal Peptide (VIP) and its receptor $VPAC_2$ are implicated in the photic entrainment and cell to cell communication among limit-cycle oscillator neurons of the SCN. In this thesis a novel model is proposed, that integrates the neuropeptide-receptor communication to the cell-level core circadian pacemaker coupling 16 neurons in a grid. It reproduces the SCN network of cells. We estimated the parameters of new coupling mechanism with a genetic algorithm, finding 27 parameter sets that produced synchrony in the rhythms of PER2 clock protein. Adding $VPAC_2$ receptor oscillations, the model displays a consistent Phase Response Curve (PRC) and achieves faster synchrony with respect to the coupled model without receptor oscillations.

Sommario

Il mammalian Circadian System é il meccanismo fondamentale responsabile del ritmo di sonno e veglia, scandendo il tempo nei ritmi biologici. Il suprachiasmatic nuclei (SCN) é una parte dell'ipotalamo ed é riconosciuto in letteratura come l'organo deputato a conferire l'intrinseco ritmo biologico che caratterizza il ritmo circadiano. É un network di neuroni, ciascuno dei quali oscilla tendendo ad un ciclo limite, caratterizzato da una specifica forma d'onda e periodo, a cui tendono ogni volta che il sistema subisce una perturbazione. In ogni sigolo neurone, attivatori e repressori della trascizione legano le sequenze target nelle regioni del promotore dei geni, generando un ritmo grazie a piú feedback loop interconnessi nell'attivazione e repressione della trascrizione. Si possono riconoscere due famiglie principali di geni coinvolti nel conferire l'oscillazione: Period (*Per1, Per2, Per3*) e Cryptocrome (*Cry1, Cry2*) la cui trascrizione é attivata da complessi eterodimerici contenenti le proteine CLOCK e BMAL. I livelli di mRNA di *Per* e *Cry* crescono. L'espressione delle proteine *Per* e *Cry* é in ritardo di diverse ore e ha un picco nel nucleo, reprimendo la trascizione dei loro stessi geni in un loop negativo. Le proteine CRY formano un complesso repressore che si associa fisicamente con il complesso *Bmal1/Clock*, inibendo la loro attivitá, nonché la trascrizione dei geni. La graduale riduzione delle PER and CRY porta una de-repressione e il ciclo riparte (Herzog 2007, Hastings et al. 2007, 2008, Weber 2009, Ukai-Tadenuma et al. 2011). L'SCN é perció composto da piú

oscillatori che comunicano per sincronizzarsi e oscillare in fase allo stato stazionario.

Il neurotrasmettitore VIP e il suo recettore $VPAC_2$ sono coinvolti nel *photic entrainment* e nella comunicazione tra i neuroni del SCN, caratterizzati dall'oscillare con un periodo che tende ad un ciclo limite di 24 ore.

In questa tesi viene presentato un nuovo modello di *cell-level circadian oscillator*, costruendo una griglia con 16 neuroni che possono comunicare per rifasarsi ed oscillare in sincronia grazie alla dinamica $VIP - VPAC_2$. Abbiamo stimato i parametri che abbiamo integrato al modello con un algoritmo genetico. Il nuovo modello é caratterizzato da un PRC consistente e raggiunge piú velocemente uno stazionario in cui i neuroni sono sincroni.

Contents

List of Figures

Introduction

Motivation

The Mammalian Circadian System plays a critical role in human life, giving it a notion of biological time. Thus, it is important to understand how circadian rhythms of physiology and behavior are coordinated in our body. Many efforts have been made to biologically investigate the genetic mechanisms and to model the mammalian circadian system.

It is accepted that the master clock is situated in the suprachiasmatic nuclei (SCN) in the hypothalamus. The pacemaker system is made up of a network of neurons, self-sustained oscillators responsible for timekeeping and entraining the rhythms from many external and internal cues. The SCN is innervated by two visual pathways, a RHT and a geniculohypothalamic tract (GHT), from where it receives the photic entrainment cues. The SCN integrates the photic and non-photic information to drive and coordinate the rhythms. It has different outputs such as circadian control over metabolism, the body temperature and hormones secretion. The core oscillator is composed of a molecular delayed feedback loop in the activations and repressions of the clock-gene transcription. Two main families of genes play a central role in the feedback loop: the *period* and the *cryptocrome*. The protein they codify for, the PER and CRY proteins, dimerize to form an heteromeric complex that physically associates with the transcription factors CLOCK and BMAL1,

suppressing their positive action on the transcription of their own *Per* and *Cry* genes. The core loop has many interlocked feedback loops in order to have precise control at many levels of the mechanism.
There has been relatively little modeling work with an appropriate level of detail to describe the communication among neurons and hence, we decided to try to address this issue.

Contribution

In the literature, there has been little effort to describe the mechanism the neurons use to communicate and entrain in order to reach a coherent oscillation at steady state. We decided to integrate the Mirsky et al. (2009) single cell model with the previously proposed VIP coupling dynamics by To et al. (2007), both presented in the Chapter 2, with the $VIP - VPAC_2$ receptor-ligand binding dynamics with $VPAC_2$ oscillations.
We simulated the neurons of the SCN using 16 cells equally spaced on a grid from random initial conditions in their phases. We estimated the new parameters of the introduced mechanism with a genetic algorithm (GA), using as a constraint that the cells should achieve a synchronized steady-state. The GA produced 27 parameter sets that led the cells to oscillate at the same phase. We defined a criterion to identify the best parameter set and we analyzed the model behavior under VIP pulse administration. We further compared the new coupled model with Mirsky et al. (2009) single cell model in combination with the To et al. (2007) coupling dynamics to see the effect of adding the more detailed receptor oscillations.

Thesis presentation

Chapter 1 presents an outline of the application of Systems Biology to the Circadian Model and I explain why understanding the Circadian Rhythm has a high social impact.

In Chapter 2, I sketch the details of the model proposed and a short comparison with main previous works.

In Chapter 3 I present the new model which is developed to extend the extant *single cell models* coupling by the $VIP - VPAC_2$ dynamic.

In Chapter 4, I present my work on the model and the results.

Finally, in Chapter 5, I draw my conclusions and discuss future challenges.

Chapter 1

Systems Biology and Chronobiology

1 Systems Biology

A new field is spreading in the bioengineering: systems biology. The key idea behind systems biology is that systems approaches such as modeling can be used to consolidate available data and knowledge and make novel predictions. The aim is not to represent molecular and chemical mechanism of the whole cell, rather to gather all the significant components involved in a process under consideration. The identification of the involved molecules is not sufficient, as one must figure out how they work together. "As systems biology emerges in the post-genomic era, the emphasis is shifting from annotation of individual genes and gene products to ascertaining how DNA-protein and protein-protein interactions occur within a complex network of structural, metabolic, and regulatory pathways in the cell" (Cassman et al. 2007). Systems biology is interested in modeling natural compounds that regulate cell functions and aims to make reliable predictions of consequences of changes in molecular properties, such as a change in particular cell function. At the

same time these investigators may desire to know the effect of properties that are less related to molecular structure, such as the affinity of the key regulatory component and its site of action.

We first need to know which are the compounds involved and to collect all the biological knowledge and assumptions on our system. The tools of molecular cell biology have greatly improved in the last two decades and they can provide a large amount of data as evidence of molecular events that can be used in new model designs. Constantly improved experiments and targeted manipulations can be practiced to investigate the effects of molecular alterations and to produce accurate data sets. It is now possible to measure the molecular interactions themselves more systematically than ever before, by screening for protein-protein, protein-DNA at high throughput, thanks to DNA microarrays to investigate changes in protein abundance and phosphorylation state, mass spectrometry and Nuclear Magnetic Resonance (NMR) to measure metabolite concentrations. Specific cell constituents can be isolated and molecular structures can be modified by in site-directed mutagenesis. Nevertheless, the main technical challenges in systems biology are on data quality and standardization. We need to make the point on the standard metric and proper annotations on public databases; new theoretical methods to characterize network topology have to be developed; more sensitive tools are required to identify and quantify the concentrations, fluxes, and interactions of various types of molecules at high resolution both in space and time; miniaturized and automated microfluidics/nanotechnology platforms, capable of parallel multiparameter analysis that integrate different operations would help to improve the measurements, joined to nanomechanical and nanoelectronic devices to improve the quantification of the forces and kinetics associated with protein/protein, protein/DNA, and protein/drug interaction.

Though the identification of the molecular components is not the limiting step anymore, lot of effort is required to formulate hypotheses on how the components interact. "The big question in biology is not regulatory linkage but the nature of biological system that allows them to be linked together in many nonlethal and even useful combinations" (Kirschner 2005). One of the first assumptions to be made when we build a model is network connection among compounds. In most of the cases, a compromise between the complexity of the reactions and of the network interactions among components and the need of a limited number of parameters in a model has to be found. A model should be kept as simple and essential as possible but rich enough to capture the dynamic we want to describe. A quantitative analysis must be developed using mathematical modeling (Lauffenburger & Linderman 1996) and sensitive analyses, to highlight the dependency of the model to parameters (Aderem 2005, *http://www.systemsbiology.org/* n.d.).

2 Mathematical modeling

"Mathematical equations are merely the language by which the hypotheses are described and their implications communicated" (Lauffenburger & Linderman 1996) and "A model is a set of structured assertions that specify the interactions among entities of a network" (Cassman et al. 2007).

Taking clues from experimental works we have to translate our assumptions in the language of the mathematics, to depict the overall model. There are different forms that a mathematical model can take, we adopt the type that mostly fits the level of accuracy and the goal of our analysis. The first main classification of a model is between a *black box* and a *white box*. The choice has to be made according to the *a priori* information available: models belonging to the first class are not very informative because they only describe the system as input, output and transfer characteristics, without regard to

the internal dynamics taking place. They can be used in the case of a lack of information. The second class is more exhaustive, it tracks the internal dynamic of the system but more knowledge about the network is assumed. According to the aim of the investigation, we will adopt the second class of model, designing a set of *Ordinary Differential Equations* (ODEs) to infer the system dynamic. Ordinary differential equations are distinguished from *partial differential equations*, which involve partial derivatives of functions of several variables to describe spatially distributed systems. The first elementary step is to draft the kinetics of the individual system reactions and the second one is to translate them in a system of ODEs. A general sketch of a system of n linear ODEs appears as in Formula 1.1:

$$\begin{aligned}
\frac{d\,x_1}{d\,t} &= a_{11} \cdot x_1 + a_{12} \cdot x_2 + a_{13} \cdot x_3 + \cdots + a_{1n} \cdot x_n + y_1 \\
\frac{d\,x_2}{d\,t} &= a_{21} \cdot x_1 + a_{22} \cdot x_2 + a_{23} \cdot x_3 + \cdots + a_{2n} \cdot x_n + y_2 \\
\frac{d\,x_3}{d\,t} &= a_{31} \cdot x_1 + a_{32} \cdot x_2 + a_{33} \cdot x_3 + \cdots + a_{3n} \cdot x_n + y_3 \\
&\vdots \\
\frac{d\,x_n}{d\,t} &= a_{n1} \cdot x_1 + a_{n2} \cdot x_2 + a_{n3} \cdot x_3 + \cdots + a_{nn} \cdot x_n + y_n
\end{aligned} \tag{1.1}$$

or in a matrix form as follows:

$$\begin{bmatrix} \frac{dx_1}{dt} \\ \frac{dx_2}{dt} \\ \frac{dx_3}{dt} \\ . \\ . \\ . \\ . \\ \frac{dx_n}{dt} \end{bmatrix} = \begin{bmatrix} a_{11} & a_{12} & a_{13} & .... & a_{1n} \\ a_{21} & a_{22} & a_{23} & .... & a_{2n} \\ a_{31} & a_{32} & a_{33} & .... & a_{3n} \\ . & & & & \\ . & & & & \\ . & & & & \\ a_{n1} & a_{n2} & a_{n3} & .... & a_{nn} \end{bmatrix} \begin{bmatrix} x_1 \\ x_2 \\ x_3 \\ x_4 \\ x_5 \\ . \\ . \\ . \\ . \\ . \\ . \\ x_n \end{bmatrix} + \begin{bmatrix} y_1 \\ y_2 \\ y_3 \\ y_4 \\ y_5 \\ . \\ . \\ . \\ . \\ . \\ . \\ y_n \end{bmatrix}$$

Where x_i, $i = 1 \ldots, n$ are the states of the system and $a_{ij}, i = 1, \ldots, nj = 1, \ldots, n$, the parameters. Since we will use the *Law of Mass Action*, and specific models of kinetics such as *Michaelis-Menten*, or *Hill-type* kinetics, our ODEs will be *non-linear* and our parameters will be the rate constants and some other kinetic parameters. Many of these rates are unknown and our aim is to "fit" them against biological data or mimicking specific real system attributes. Intrinsic variability among cells existing in nature is simplified. We assume homogeneity of our data and the model we are going to fit is an average individual of the heterogeneous population. Chemical reactions and molecular collisions are random events by its own nature and the model we are drawing is neglecting this randomness. It is a *deterministic* model, against the *stochastic* approach that indeed considers the variability. Stochastic modeling is a tool for estimating probability distributions of potential outcomes by allowing for random variation in one or more inputs over time (Fall et al. 2002, Edelstein-Keshet 2005, Murray 2007, Polynikis et al. 2009, *http://www.systemsbiology.org/* n.d.).

3 Circadian Rhythms

Periodic wheel running activity in mice, daily leaf movements of light sensitive plants such as the Mimosa (de Mairan 1729), bees returning to a feeding table at a fixed time of day, periodic states of vigilance and rest, hormone secretion, liver activity, they are all examples of 24-h rhythmicity. The *circadian clock* is the intracellular system responsible for the timekeeping that allows organisms to anticipate daytime and hence to coordinate their physiology to the geophysical time. It is a complex network of genes and proteins with interconnected mechanisms, which are still incompletely understood. Until a century ago, the existence of an internal timekeeping was ignored and the notable cyclic events in nature were justified as passive responses to the exogenous stimuli of the environmental cycles. Early circadian pioneers experimented on plants circadian activity. The first example was a short communication addressed to the Royal Academy of Science in Paris in 1729, where the French astronomer Jean Jacques d'Ortous deMarian tested Mimosa leaf rhythms in darkness, without cyclic environmental information, observing the persistence of movements. The idea of an intrinsic clock was abandoned questioning whether persistent daily rhythms under so-called constant condition was only the failure to eliminate other potential clues, like barometric pressure cycles or temperature variations. A true interest in chronobiology spread in the 20^{th} century when Colin S. Pittendrigh and Jurgen Ashoff started their studies on internal clocks gating pupal hatching rhythms in insects and on the daily locomotor activity rhythms of mice. The first symposia among different laboratories working on circadian rhythm, was in New York in 1960 and many others followed. In this contest Pittendrigh gave a significant lecture whose title was: "Circadian Rhythms and the Circadian Organization of Living Systems", that stands as a symbolic charter to this day. It drew the phylogenetic breadth of in-

ternal timing organisms and the ecological significance of living clocks at all levels of physiological organization. In this context, Pittendrigh presented the formal defining properties of circadian rhythms still accepted today. The first breakthroughs were the discovery of an insect pacemaker in 1968 and the recognition of the suprachiasmatic nuclei (SCN) as circadian mammalian pacemaker in 1972. As parallel processes, the interest in the chronobiology increased, the knowledge and understanding of the subject spread, and a new technical terminology was coined to depict experiments and discoveries. An example is the common jargon for the lighting schedules used and rhythm concepts. A small dictionary of the most common words follows:

- L refers to lights on.
- D to darkness.
- LL to constant light.
- DD for constant dark.
- LD n:m is the ratio of hours of light to dark on a day-night schedule as, to indicate n hours of light, followed by m hours of dark.
- *Circadian Time (CT)* is subjective internal organism time in which one circadian period length is divided into 24 equal parts, each a circadian hour. By convention CT 0 corresponds to subjective dawn and CT 12 to subjective dusk.
- *Actogram* and *actograph* are both graphs of the daily activity.
- *Free run* is the state of an oscillator when not influenced by any external cues.
- *Free running period (FRP)* is the period length of a biological oscillator.
- *Photic entrainment* and *Nonphotic entrainment* are respectively the entrainments brought about by the action of a light cycle and of a free running rhythm by environmental cycles other than light.

- *Zeitgeber* (from German for "time giver", or "synchronizer") is any exogenous (external) cue that synchronizes an organism's endogenous (internal) time-keeping system (clock) to the earth's 24-hour light/dark cycle.
- *T-cycle* is the cycle of an entraining agent, or time giver.
- *Phase response curve (PRC)* is a map of the phase dependent resetting- that is, the phase-dependent response of a circadian clock to an entraining agent delivered at different times through a circadian day.
- *Cell-autonomous* Intrinsic to a single cell. Circadian rhythm generation and output is a property of circadian pacemaking cells.
- *Clock genes* a class of genes, the primary function of which is to participate in a transcription-translation negative-feedback mechanism that generates a near 24-hour rhythm in physiology.

Many models have been drawn so far: of the *Molluscus Bulla* and *Aplysia*, of *Arthropods*, of the fruitfly *Drosophilia* and of the fungus *Neurospora*, of the *Arabidopsis*, of fishes and reptiles. Our major interest is in the mammalian models.

3.1 Mammalian Circadian Rhythm: Social impact

The Circadian System plays a critical role in human life. We can appreciate how much our life is centered on circadian variation just thinking of the daily performance rhythms. Alertness and mental performance show circadian patterns. There are different studies demonstrating that people are more disposed towards and efficient in complex tasks in late morning and on tests involving visual search in late afternoon, even if these kinds of performances can be strongly susceptible to the environmental noise and conditions and are affected by the influence of fatigue, thus difficult to be objectively conducted (Takahashi & Arito 2000, Dunlap et al. 2003). The field of sleep

research overlaps with the circadian field, since molecular understanding of the mechanisms governing the sleep-wake cycle can improve the therapies for sleep diseases. Sleep deficiency affects millions of people and is strictly related to industrial and car accidents (Connor et al. 2001). Sleep debt impairs cognitive functions (Thomas et al. 2000), increases the severity of obesity, diabetes (Knutson et al. 2007) and hypertension (Gangwisch et al. 2006) and aggravates many health conditions of the elderly (Latta & Van Cauter 2003, Colten & Altevogt 2006).

3.2 Mammalian Circadian Rhythm: Physiology

The circadian timekeeping system has a hierarchical architecture in which every clock is an oscillatory system. These biological oscillators can be divided into pacemakers and damped or slave oscillators. Pacemakers are self-sustained oscillators that must synchronize to generate a common output and to achieve a coherent rhythm. Damped and slave oscillators cannot sustain a rhythm by themselves and they are under the pacemakers' control, that regulate their phase period and amplitude. In mammals, circadian rhythms of physiology and behavior are generated and coordinated by a master clock that resides in the suprachiasmatic nuclei (SCN) of the hypothalamus even if many self-sustained oscillators have been found in several tissues throughout the body. These non-central self-sustained oscillating structures are called "peripheral oscillators". It is hypothesized that these peripheral oscillators might have the control over local rhythms, observing what happens in the lungs and in the liver. Owing to the paracrine and the synaptic communication of SCN cells, the SCN oscillators never desynchronize in animals deprived of external timing cues. They are limit-cycle oscillators, characterized by a standard waveform and period to which they return every time after a perturbation occurs.

The list of daily circadian behavior, physiological, and biochemical phenomena is very long. Neuronal projections from SCN are well placed to drive endocrine and other circadian cycles (Hastings et al. 2007). Among these, a notable example can be provided by the metabolism and the way it switches between repairment processes in nocturnal hours and diurnal processes to support energy burn; others are body temperature variations or melatonin levels. Also the secretion of hormones is temporally precise and periodic, oscillating over hours, days, months, coordinated, modulated and driven by the SCN (Maywood et al. 2007). These rhythms must be synchronized with external environmental cues and SCN modulates entrainment responding to a variety of signals. Several stimuli are capable of entraining the oscillator to their phase, among these are food availability, social contacts, temperature but the most remarkable is the light/dark cycles. SCN response is a wide spectrum of signals, ranging from humoral signals such as melatonin of the pineal or hormones of the pituitary gland to neuronal connections. Studies of locomotor activity rhythms and testicular responses of Syran hamsters exposed to light/ dark cycle of different resonances provided the first evidence for a circadian basis of photoperiodic time measurement in a mammal (Dunlap et al. 2003). Further proof of the SCN being the master clock comes from experimental data where all SCN afferent and efferent nerves were cut with a knife *in vivo* preparation or similarly isolated by electrolytic or chemical lesions. All the experiments showed a correlation of the isolated hypothalamic island with a loss of overt circadian rhythm. Explant cultures and dispersed-cell cultures experiments lend further proof as a persistance in free-running rhythms is detected (Ciarleglio et al. 2009).

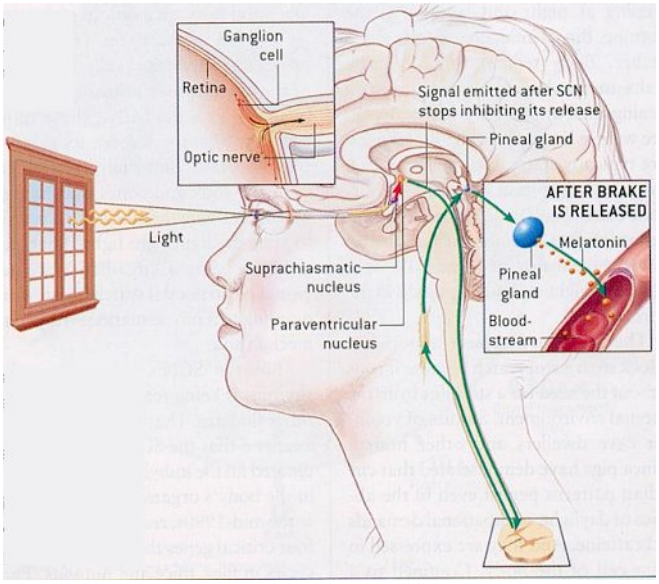

Figure 1.1: Structure of the SCN from *http://universe-review.ca/* (n.d.).

The SCN is made up of two functionally and anatomically separated parts: the core, or ventrolateral area (VL-SCN), and the shell, or dorsolmedial area (DM-SCN). Both the portions are small packed clusters of nerve cells, placed above the optic chiasm in the anterior ventral hypothalamus, but they can be distinguished by their different neurochemical and cytochemical characteristics: the VL-SCN receives inputs from the retinohypothalamic tract (RHT) axonal projections and it responds synthesizing vasoactive intestinal polypeptide (VIP) and gastrin-releasing peptide (GRP), while the DM expresses arginine vasopressin (AVP) and calretinin neurons in response to input from hypothalamus and limbic areas, as well as from the VL-SCN (Dunlap et al. 2003). The SCN is innervated by two visual pathways, a RHT and a geniculohypothalamic tract (GHT). Input for entrainment comes primarily through specialized retinal ganglion cell photoreceptors, which connect through the retinal hypothalamic tract to the SCN. The failure of entrainment when the SCN is severed from the optic chiasm by knife cut procedures, reveals its

function. Indeed in light-dark cycle, the lesioned animals exhibit free running rhythms (Brown & Piggins 2007). Previous experiments showed evidence that GHT is not necessary for entrainment (Johnson et al. 1988). Glutamate neurotransmitter is released from RHT as main photic input to SCN (Golombek & Rosenstein 2010). Also aspartate, PACAP and GABA are found to have a significant role in photic response. It is nevertheless true that several experiments suggest that glutamate conveys the most of photic information. Pieces of evidence are deduced with optic nerve stimulation and light or electrical stimulation that induce glutamate released (Brown & Piggins 2007). Different glutamatergic receptors have been found in the SCN as NMDA, AMPA and metabotropic types. Since NMDA receptor is found to exhibit a change in SCN, this can be translated in a gating of photic information and in a first step of entrainment (Golombek & Rosenstein 2010).

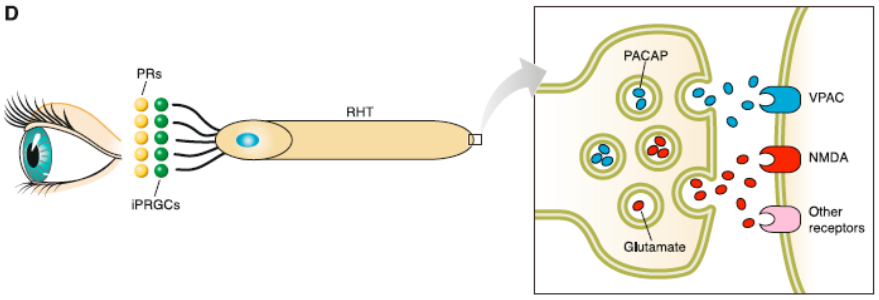

Figure 1.2: Schematic representation of the retinohypotalamic tract, originating in the retinal ganglion cells and innervating the ventral part of SNC. Figure from Golombek & Rosenstein (2010).

3.3 Mammalian Circadian Rhythm: Modeling the system

The rise of biochemistry, metabolic engineering and molecular biology lead researchers to make and test different hypothesis on how the “clock” works.

One of the first models theorized for the 24 hours rhythm was given by a delay of expression, transcription and translation of a group of hundreds of genes. These genes and their expressed protein were linked within a network in a closed loop in which the level of every protein is used to upregulate the transcription of another gene. Many models arose accompanied by new understandings of the molecular bases for the circadian rhythmicity, improving the level of detail of the model and its predictive power. The discovery of the clock genes enabled us to identify the molecular machinery necessary to generate circadian rhythms; they act to generate circadian transcriptional oscillations through a regulatory system comprised of negative feedback loops. Three main properties characterize the system: endogenous oscillations with an approximately 24-hours period, the entrainment to external environmental changes (light and temperature), and the temperature compensation over a wide range (Golombek & Rosenstein 2010).

We can *in silico* design the clock of a multi-cellular organism at different levels: the *molecular clock* describes the core mechanisms of the transcriptional and post-transcriptional network, at tissue or single neuron levels. The *central clock* at the cellular level describes the communication among cells by the cellular coupling, modeling the signal transduction and giving an outline of the intercellular network. It takes into account the distinction between peripheral and central clocks (Golombek & Rosenstein 2010). We will give here details of the molecular clock to focus more on cell to cell communication in Chapter 2.

The oscillation of the molecular clock is governed by three clock-controlled DNA cis-elements: morning (E-box/E'-box or E/E' box: CACGT[G/T]), daytime (D-box:TTA[T/C]GTAA) and night-time (RevErbA/ROR binding element, or RRE: [A/T]A[A/T]NT[A/G]GGTCA). A sketch of the network is provided in Figure 1.3:

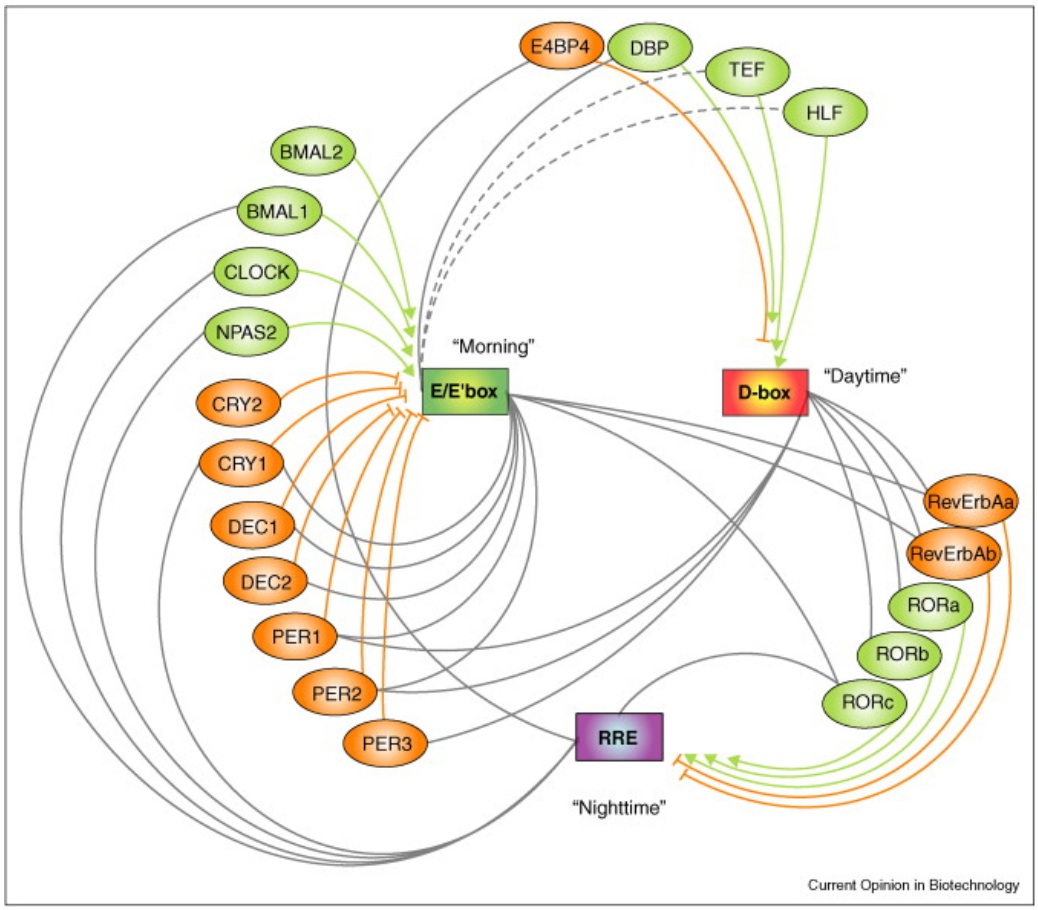

Figure 1.3: Overview of the transcriptional network of the mammalian circadian clock. Genes, CCEs, transcriptional/translational expression, activation, and repression are depicted as ovals, rectangles, grey lines, green lines, and orange lines, respectively. The E-box-mediated transcription program is directly or indirectly controlled by at least 11 transcription factors. These include four basic helixloophelix (bHLH)-PAS transcription activators, Clock, Npas2, Bmal1 (also known as Arntl or Mop3), and Bmal2; three Period genes, Per1, Per2, and Per3; two Cryptochrome transcription repressors, Cry1 and Cry2; and two other bHLH transcription factors, Bhlhb2 and Bhlhb3 (also known as Dec1 and Dec2). At least four bZIP-family genes, Dbp, Hlf, Tef and E4bp4 (also known as Nfil3), and five orphan nuclear hormone receptors, Nr1d1, Nr1d2 (also known as RevErbAα, RevErbAβ), Rora, Rorb and Rorc, control the D-box- and RRE-mediated transcription programs, respectively. From Susaki et al. (2010)

.

It is a highly interconnected network in which transcriptional activators (green in the figure) and repressors (orange in the figure) bind target sequences in the promoter regions (colored boxes) of the genes. The expression pattern of each gene is determined by its complement of different promoter elements. In the figure we can see connections among genes and promoters depicted with gray lines. The E/E' box-mediated transcriptional program is crucial because it is the more interconnected node. The rhythmicity is generated by the feedback loops of activations and repressions of clock-gene transcriptions. Recent investigations revealed that post-translational regulation of the clock proteins is crucial for the functioning of the molecular oscillator and for precise temporal control of the circadian transcription. The central factors in this model are two genes families: Period (*Per1, Per2, Per3*) and Cryptocrome (*Cry1, Cry2*) which transcriptions are activated at the beginning of the circadian day by heteromeric complexes containing CLOCK and BMAL1 proteins, acting through the E-box sequences. *Per* and *Cry* mRNA levels accumulate over circadian daytime. *Per* and *Cry* proteins expression is delayed by several hours and peaks in the nuclei at the end of the circadian day, repressing their gene transcription in a negative feedback loop. CRY proteins form repressor complexes that physically associate with *Bmal1/Clock* complex, inhibiting their activity thus inhibit the E/E' box mediated transcription. Gradual loss of PER and CRY proteins leads to de-repression, and then the daily cycle starts anew (Ukai-Tadenuma et al. 2011, Herzog 2007, Hastings et al. 2007, Weber 2009, Hastings et al. 2008). More detailed models will be presented in Chapter 2.

Chapter 2

Mammalian circadian models

1 Detailed mathematical circadian models

As related in advance in Chapter 1, recent discoveries have shed a great deal of light on the molecular mechanism that generates the circadian rhythms displayed in many living organisms. I am giving details on three of the main computational models for the mammalian circadian clock emerging from these experiments, which my work is based on. The first one is Leloup and Goldbeter's model (Leloup & Goldbeter 2003), the second is Mirsky *et al.* model (Mirsky et al. 2009) and the third is To *et al.* model (To et al. 2007).
All the models presented from the literature lack of detailed modeling of the $VIP-VPAC_2$ receptor-ligand binding and cascade. We will explore the role of this fundamental neurotransmitter-receptor communication among neurons, how a receptor-ligand dynamic can be mathematically modeled and we will elucidate the solution we found to integrate that mechanism to the mammalian circadian model.

1.1 Leloup and Goldbeter model

The Leloup and Goldbeter's model is a deterministic tissue level model that means that the data they used for building their model were collected from a whole tissue, not from a single cell neuron. It uncovers the possible existence of multiple sources of oscillatory behavior. It incorporates the negative autoregulation of genes expression (*Per, Cry, Bmal1, Clock* and *Rev-Erbα* genes, PER1, PER2, PER3, CRY1, CRY2, BMAL1, CLOCK and REV-ERBα proteins) and post-translational regulation of the proteins involved by reversible phosphorylation, and light induced *Per* expression. It is a 19 state model that describes the following molecular processes:

- *Per, Cry, Bmal1* gene transcription and mRNAs degradations in the nucleus, simplifying the model with no distinctions among *Per1, Per2, Per3*, all considered as *Per*, and similarly for *Cry1, Cry2*, represented as *Cry*. *Per* and *Cry* transcription is activated by CLOCK-BMAL1 complex transcription factor. The effect of light is to enhance the *Per* transcription and is considered as governing the value of the maximum rate of *Per* expression.
- mRNA translation in the cytosol to produce unphosphorylated proteins PER, CRY, BMAL1.
- Reversible phosphorylation of the PER, CRY, BMAL1 proteins in the cytosol and their degradation.
- Formation of the cytosolic unphosphorylated PER-CRY complex and its degradation.
- Reversible phosphorylation of PER-CRY complex, its entry in the nucleus, its reversible phosphorylation in the nucleus and its degradation.
- Reversible entry of BMAL1 protein in the nucleus, reversible phosphorylation and degradation.

- CLOCK protein level is considered in equilibrium and its constant level is a parameter.

- They assume fast equilibrium in the formation of complex between unphosphorylated BMAL1 and CLOCK in the nucleus. The limiting agent is the unphosphorylated BMAL1 level and the complex dose is equal to the unphosphorylated BMAL1 availability in the nucleus. This complex plays a significant role in the nucleus because it activates *Per* and *Cry* gene transcription.

- They model the formation of the inactive complex by PER-CRY binding CLOCK-BMAL1. CLOCK-BMAL1 complex is not a promoter anymore on *Per* and *Cry* genes so PER and CRY protein are in a negative feedback on their production.

- In analogy with PER and CRY negative autoregulation, BMAL1 protein is involved in an indirect negative feedback on its gene transcription. BMAL1 is a transcription factor for *Rev-Erbα* gene which protein, REV-ERBα, represses the expression of *Bmal1*.

The model represents an autonomous sustained oscillation in DD and the entrainment of the light. It predicts an antiphase relationship between *Per* and *Cry* mRNAs and *Bmal1* mRNA, as experimentally demonstrated. *Rev-Erbα* mRNA oscillates in phase with *Per* and *Cry* mRNAs, as observed in the Figure 2.1:

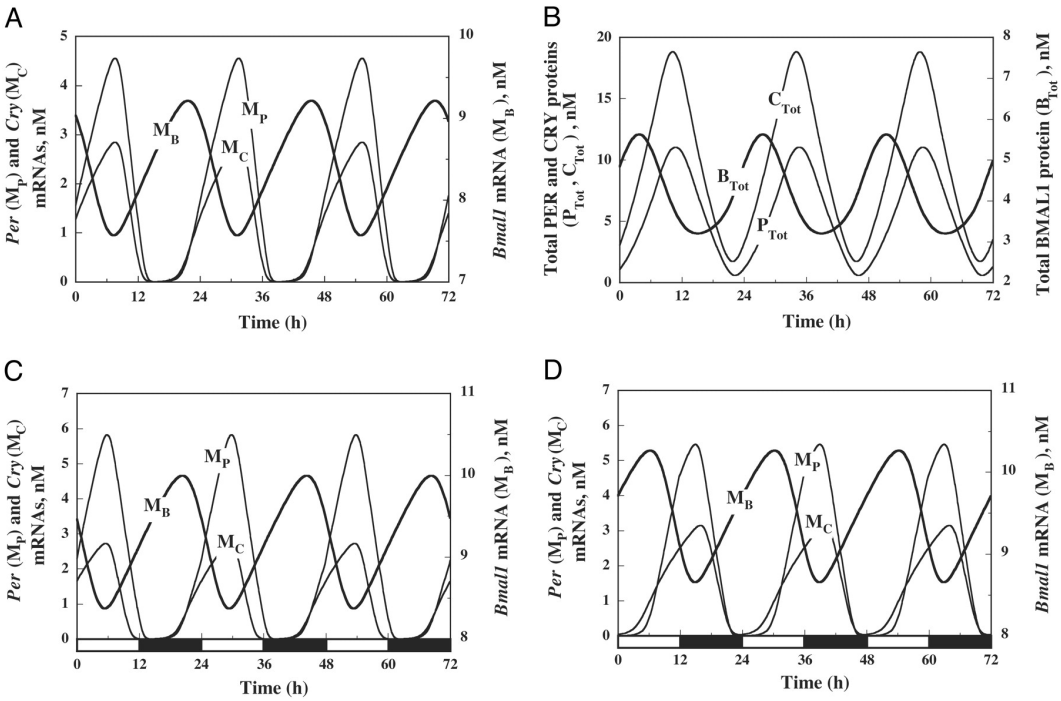

Figure 2.1: Circadian oscillations in DD (A and B) and entrainment by LD cycles (C and D). (A) The mRNA of Bmal1 oscillates in antiphase with respect to the mRNAs of Per and Cry.(B) Corresponding oscillations of the PER, CRY, and BMAL1 proteins. (C) Oscillations of the mRNAs after entrainment by 12:12 LD cycles. The peak in Per mRNA occurs in the middle of the light phase. (D) Oscillations are delayed by 9 h and the peak in Per mRNA occurs in the dark phase when the value of parameter K_{AC} is decreased from 0.6 to 0.4 nM. Other parameter values correspond to the basal set of values listed in the Supporting Text of Leloup & Goldbeter (2003). The curves have been obtained by numerical integration of Eqs. 116 (see Supporting Text of Leloup & Goldbeter (2003)) of the model without REV-ERBα. Figure from Leloup & Goldbeter (2003).

A sketch of the model is provided in Figure 2.2:

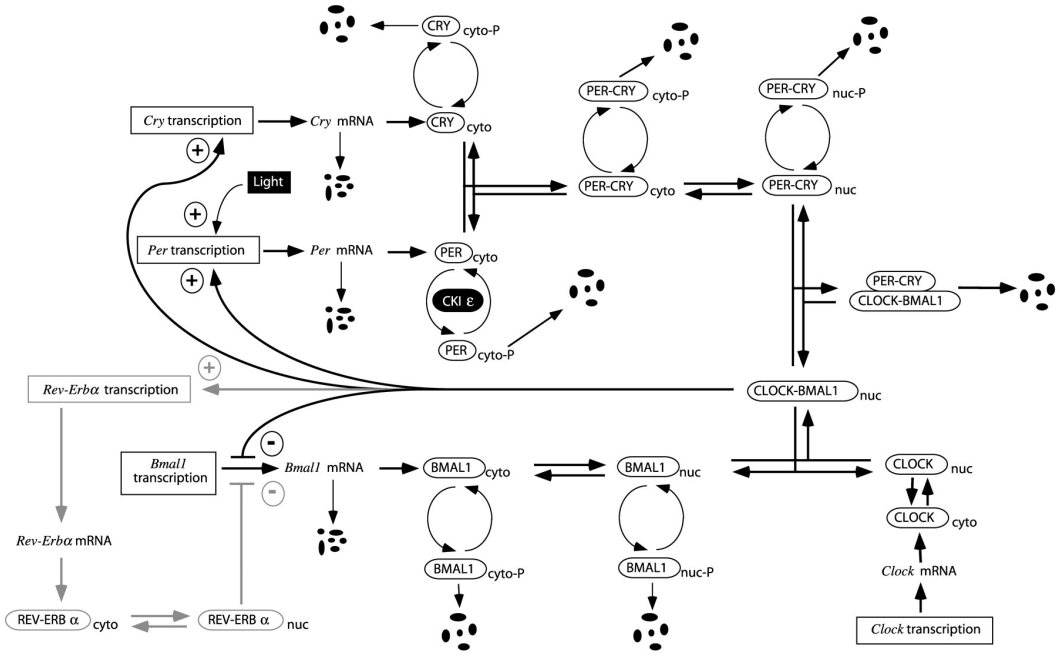

Figure 2.2: Sketch of the Leloup and Goldbeter mammalian model, with indication of the kinetics parameters. Figure from Leloup & Goldbeter (2003).

1.2 Mirsky *et al.* model

While Leloup and Goldbeter (Leloup & Goldbeter 2003) is a tissue level model, Mirsky *et al.* model (Mirsky et al. 2009) highlights cell-autonomous circadian phenotypes using cell-level data. This is a more detailed model, considering the different types of *Per* genes and *Cry* genes, adding states for each *Per1, Per2, Cry1, Cry2* genes and related PER1, PER2, CRY1 and CRY2 proteins. It also includes the *Rev-Erbα* interlocking loop. The resulting mathematical model has 21 states and 132 parameters. They assume *Michaelis-Menten* kinetics for transcriptional rates and mass action kinetics with *Michaelis-Menten* and *Hill* forms for all other rates. They used an evolutionary procedure to derive the parameter set, because of the unreliability of the experimental data, and evaluated the model against desired phase rela-

tionship between oscillatory profiles of the components. The model was validated to see whether *in silico* knock-out genes and constitutive production of proteins could predict the phenotypes of the cell-autonomous experimental data. The model correctly predicts the available biological evidence. They also validate the model against knock-out phenotype robustness to parameter perturbation. Changing parameter above the value of 10% from their nominal value, the retention of rhythmicity is reduced; below this perturbation phenotype is conserved for all the knock-out. A sketch of the genes regulatory scheme and of the network diagram used to draw the model is depicted in Figure 2.3:

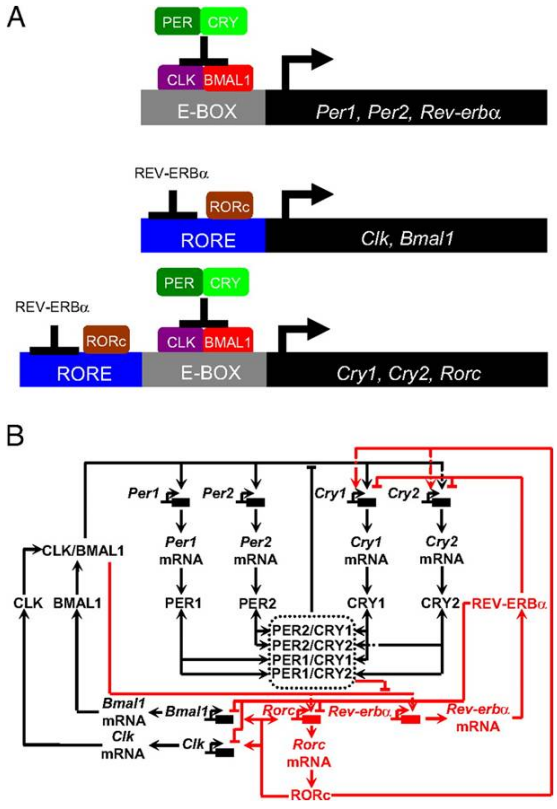

Figure 2.3: Mirsky *et al.* model: A) genes regulatory scheme. B) network diagram. Figure from Mirsky et al. (2009).

1.3 To *et al.* model

The To *et al.* model (To et al. 2007) incorporates a multicellular mechanism to achieve synchrony among heterogeneous oscillators. It focuses on intercellular coupling and its robustness and network properties. Biological advances in the understanding of the molecular basis for circadian rhythms highlight that multiple clocks can synchronize and can communicate through the neurotransmitter VIP and its receptor $VPAC_2$. They further report that the robustness in timekeeping precision arises from the collective behavior of the coupled system, not at single-cell level. The intercellular mechanism is not well understood and we will focus on $VIP-VPAC_2$ molecular details in the section 2.

To *et al.* implemented a core oscillator from Leloup and Goldbeter's model (Leloup & Goldbeter 2003), incorporating the coupling mechanism between cells. It does not include 3 states of the Leloup and Goldbeter's model that involve REV-ERBα feedback loop, resulting in a 16 state model instead of 19 states. It also assumes a different mechanism for light entrainment that involves elevation of intracellular calcium, protein kinase activation, cAMP and binding of phosphorylated CREB to mediate *Per* gene transcription, modulating the oscillator phase. To *et al.* include also in the model the neurotransmitter VIP. $VPAC_2$ receptor is considered as constitutively expressed, with no mRNA modeling. Further assumptions have been chosen following the experimental evidence that VIP release in the SCN is circadian, influenced by light that increased its level, and correlated with the circadian intercellular calcium level. Its release is modeled at single cell level and high enough to saturate $VPAC_2$ receptor under the increasing light effect. It is circadian during darkness, in phase with *Per* mRNA as follows:

$$\rho_i = a\frac{M_{P,i}(t)}{M_{P,i}(t)+b} \tag{2.1}$$

where ρ_i is the extracellular concentration of VIP produced by the i-th cell

and $M_{P,i}$ is the *Per* mRNA concentration in the i-th neuron, a is the maximum VIP release and b is the saturation constant. Cells heterogeneity is implemented as different level of VIP seen by each cell, and the N cells in the network are represented as N nodes equally spaced in a grid. The VIP level seen by every neuron is the weighted VIP produced by the other neurons in the grid. Its mathematical expression is:

$$\gamma_i(t) = \frac{1}{\epsilon} \sum_{j=1}^{N} \alpha_{ij} \rho_j(t) \tag{2.2}$$

where

$$\epsilon = \frac{1}{N} \sum_{i=1}^{N} \sum_{j=1}^{N} \alpha_{ij} \tag{2.3}$$

where $\gamma_i(t)$ is the local VIP seen by neuron i, α_{ij} is the weighted effect of neuron j on neuron i, reciprocally proportional to the distances between cells, assuming a unit distance between neighbors. VIP acts binding the monovalent $VPAC_2$ receptor reversibly, as rapid as to be assumed in equilibrium. The complex formation is modeled as:

$$C_{eq} = \frac{R_T \gamma}{K_D + \gamma} \tag{2.4}$$

Where R_T is the total surface receptor density, assumed to be constant, K_D is the equilibrium dissociation constant for the formation complex reaction. They will consider β as the fraction of the complex density C_{eq} over the total reception density R_T, so that β can vary between 0 and 1:

$$\beta = \frac{\gamma}{R_D + \gamma} \tag{2.5}$$

The VIP and the light act additively on calcium level, increasing its release respectively from ligand-sensitive pool and from light-sensitive pools, the

extent is proportional to β and δ respectively. Calcium is assumed to be at steady-state, with an influx of extracellular Ca^{2+} depicted as v_0 and efflux rate represented as k:

$$k\, Ca^{2+}_{Cytosol} = v_0 + v_1\beta + v_2\delta \tag{2.6}$$

Cytosolic calcium level activates CREB via a *Michaelis-Menten* process, affecting the maximum rate of kinase v_k:

$$\mathrm{v}_k = V_{MK}\frac{Ca^{2+}_{Cytosol}}{K_a + Ca^{2+}_{Cytosol}} \tag{2.7}$$

where V_{MK} is the maximum rate of activation by Ca^{2+}, K_a is a threshold constant. The explicit role of v_s appears in time variation of the fraction of CREB in phosphorylated form, depicted as CB^*:

$$\frac{d\,CB^*}{d\,t} = \Big(\frac{v_P}{CB_T}\Big)\Big[\Big(\frac{v_K}{v_P}\Big)\frac{1 - CB^*}{K_1 + (1 - CB^*)} - \frac{CB^*}{K_2 + (1 - CB^*)}\Big] \tag{2.8}$$

where v_P is the maximum rate of phosphatase activity, CB_T is the total amount of CREB, K_1 and K_2 are threshold constants. CREB is a transcription factor for the *Per* gene and its binding is modeled as the formation of the $VIP - VPAC_2$ complex. The same way they found β, here they model λ as the extent of CREB activation:

$$\lambda = \frac{CB_T CB^*}{K_C + CB_T CB^*} \tag{2.9}$$

where K_C is the dissociation constant. The last step of the cascade is the *Per* mRNA transcription rate v_{sP}, that is modeled as the sum of a basal transcription rate v_{sP0} and the effect of phosphorylated CREB:

$$v_{sP} = v_{sP0} + C_T\lambda \tag{2.10}$$

where C_T is the scaled-maximum effect of the CREB-binding element on the *Per* gene. The *Per* mRNA transcription rate v_{sP} is incorporated into the

kinetic equations of the gene regulation model. The To *et al.* model differs from the 16 state Leloup and Goldbeter model due to the additional differential equation and 5 algebraic equations just presented above.
The model has been evaluated against the experimentally observed data where a heterogeneous cell ensemble requires VIP to communicate, entrain and synchronize. They used this model to test the robustness of the network, the influence of the VIP and of cell heterogeneity in the synchronization. They perturbed the model parameters to model the biological heterogeneity among cell. They found that rhythmic release of VIP helps cells to couple and that, despite a slow desychronization under constant light condition, the network achieves a fast resynchronization with VIP pulses. Even if the molecular cascade that follows the VIP binding $VPAC_2$ is very simplified, the model can predict the experimentally observed behavior. It suggests that the VIP is a critical element in cells coupling and in the network synchronization.

2 $VIP - VPAC_2$ coupling and the VIP cascade: physiology

SCN neurons in a network show a synchronized rhythm activity while low density cultures fail to synchronize. Individual SCN neurons can generate circadian oscillations, some fully isolated cells can sustain circadian cycling for at least one week and both rhythmic and arrhythmic neurons express VIP neuropeptide. This suggests that neurons' synchrony is due to synaptic communication between them that allows intercellular interaction and coordination, necessary to stabilize their otherwise noisy cycling (Webb et al. 2009). Despite recent advances in the field, it is unclear how they maintain the rhythm and synchronize *in vivo* and how the temporal information is communicated (Aton et al. 2005). Many neuropeptides and neuro-

transmitters have been found to be abundant in SCN cells. We can identify some of them as responsible for intracellular communication and synchrony: the vasoactive intestinal polypeptide (VIP), the pituitary adenylate cyclase-activating polypeptide (PACAP), the gastrin-releasing peptide and the gamma aminobutyric acid (GABA) (Kamaishi et al. 2004, Aton et al. 2006, Ospeck et al. 2009). We will focus our attention on the VIP and its receptor $VPAC_2$.

The vasoactive intestinal polypeptide is a neuropeptide in the secretin superfamily, synthesized from prepoVIP where the breaking of a chemical bond results in both VIP and peptide histidine isoleucine. The latter is abundant and co-localized with VIP and, in rodents, PACAP, VIP and peptide histidine isoleucine show 68% of homology (Piggins & Cutler 2003). These three peptides bind with almost the same affinity the $VPAC_1$ and $VPAC_2$ receptors, while PAC_1 receptor preferentially binds only PACAP. The $VPAC_2$ is a G-coupled receptor, that is known to be linked to the stimulating ganine nucleotide binding protein (G_s) and adenylyl cyclase (AC), with cyclic AMP (cAMP) (Hao et al. 2006).

An abundance of VIP-binding sites in rodents SCN has been detected by radioligand studies, in regions close to an intense immunostaining of VIP. They further confirmed a heavy expression of $VPAC_2$ mRNA with *in situ* hybridisation investigation. Evidences of the complex formation and abundance of the components in the SCN led to the hypothesis of the fundamental role of the $VIP - VPAC_2$ in the circadian system (Piggins & Cutler 2003). The loss of VIP or $VPAC_2$ tested by Colwell *et al.*, results in functionally similar deficits in both behavior and SCN firing rhythmicity and their data provided evidence that $VIP - VPAC_2$ signaling was responsible for the synchrony among neurons and in maintaining circadian rhythmicity (Aton et al. 2005). Using real-time bioluminescence imaging of cellular circadian gene expression

in SCN slice cultures, Hastings *et al.* (Maywood et al. 2006) demonstrated that interneural VIP-ergic signaling through its receptor $VPAC_2$ is necessary to confer synchronization of the intracellular molecular timekeeping. They used Vipr2 lacking mutant mice, the gene encoding for $VPAC_2$ receptor, and recorded circadian gene expression of $Vipr2^{-/-}$ mutant mice carrying *mPer1::luciferase*. They compared the time patterns of this circadian clock gene marker with the wild type control bioluminescence: low signal amplitude and no circadian time series were detected in the mutant mice, providing evidence that $VIP - VPAC_2$ signaling is essential (Maywood et al. 2006). Futher anatomical studies indicated that VIP and $VPAC_2$ receptor are both expressed in light sensory circuit: photic information is driven through the retinohypothalamic tract (RHT) to the SCN. Many VIP-expressing cells in the ventral SCN receive photic information from RHT. These neurons are contacted by RHT terminals and this suggests a relation between photic inductions and VIP signalling cascade (Dragich et al. 2010). The observation that VIP neurons interface incoming environmental information from the retinal efferent input induced many functional studies to investigate VIP role in photic entrainment. In order to test whether VIP-$VPAC_2$ is responsible for gating photic input, Hughes et al. (2004) used immunohistochemical detection of pERK and cFOS in mutant mice lacking $VPAC_2$ receptor. pERK and cFOS are indeed robust markers of SCN neuronal photic activation, being part of intracellular modulating cascades that mediate the action of light on the rodent SCN pacemaker. Levels of pERK and cFOS have been shown to be circadian in the wild type rodents under LD and DD cycles, with high levels during subjective day phase and low levels during subjective night phase. The loss of circadian expression of these markers in the $VPAC_2$ altered phenotype mice reveals a dysfunctional circadian oscillator. It was expected to have an increase of pERK and cFOS levels in constant

darkness during subjective night but not during subjective day, in response to light pulses in the wild type mice. In contrast, an increased expression of the markers was detected in mice lacking the $VPAC_2$ receptor both during subjective day and night, as additional evidence of loss of aberrant gating of photic input of mutants (Hughes et al. 2004). Shinohara et al. have determined by enzyme immunoassay the daily and circadian VIP concentration and by in situ hybridization histochemistry the temporal profiles of its precursor mRNA and its receptor mRNA. Neither VIP mRNA, $VPAC_2$ mRNA nor VIP patterns show circadian rhythms in constant darkness (DD) but they were all responsive to light, decreasing over the period of light exposure, suggesting a role in the mediation of photic input (Shinohara et al. 1993, 1999, Itri & Colwell 2003*a*). Mice carrying null mutation of the receptor fail to exhibit circadian expression of the core clock genes *mPer1, mPer2* and *mCry1* (Harmar et al. 2002) and are arrhythmic at the molecular, neurophysiological and behavioral levels (Piggins & Cutler 2003). Dragich et al. (2010) reported an altered photic regulation in mice deficient in either VIP or PACAP and that VIP, but not PACAP, is necessary for the appropriate temporal gating of light-induced clock gene *Period1* expression. They also recorded patch-clamp in an acute brain slice preparation to test the influence of the influence of bath-applied VIP. VIP treatment evoked the same phase-shift on behavioural rhythms that was detected with short light pulses administered to rodents during the early or late subjective night. This confirms the theory that VIP is an intermediate in the process of entraining the circadian system to light pulses (Itri & Colwell 2003*b*). Vosko et al. (2007) pointed out the role of VIP, "We believe that VIP:

- acts as a major synchronizing agent among SCN neurons
- modulates the molecular oscillations within individual oscillators and
- synchronizes SCN neurons with light cues"

and they provide a summary of the state of art in understanding the role of VIP (Vosko et al. 2007).

Many efforts have been made to investigate the $VIP-VPAC_2$ signal transduction pathway from the receptor binding ligand to its final effect on *Per1* gene expression and in phase-shifting the circadian clock oscillation. Hao et al. (2006) have developed a kinetic model integrating cyclic AMP (cAMP) accumulation, protein kinase A (PKA) activation, cAMP-response element binding protein phosphorilation (CREB) and *Per1* induction (Hao et al. 2006). The same signaling cascade pathway is assumed by Rusnak et al. (2007). We are interested in integrating the mammalian circadian model with the $VIP - VPAC_2$ dynamics and we want to investigate the effect of the communication among cells dues to VIP coupling, on neurons' synchrony.

3 Mathematical modeling for receptors

To model $VIP - VPAC_2$ mechanisms, we need to elucidate the possibilities for mathematical modeling of receptors. To gain an insight into the relationship between receptor/ligand molecular properties and the cell function they govern, it is advisable to combine cell biology experimentation and quantitative engineering models. Based on the data produced altering receptor and ligand properties, we can validate the model and exploit its predictive power. In cell biology a receptor is a structure on the surface of the cell (or inside a cell) that selectively receives and binds a specific substance (*http://www.medterms.com/* n.d.). There are also intracellular receptors but we will focus on the cell surface receptors to narrow the scope of molecular components to be considered later. There are many receptors, for a wide range of functions and of binding ligand.

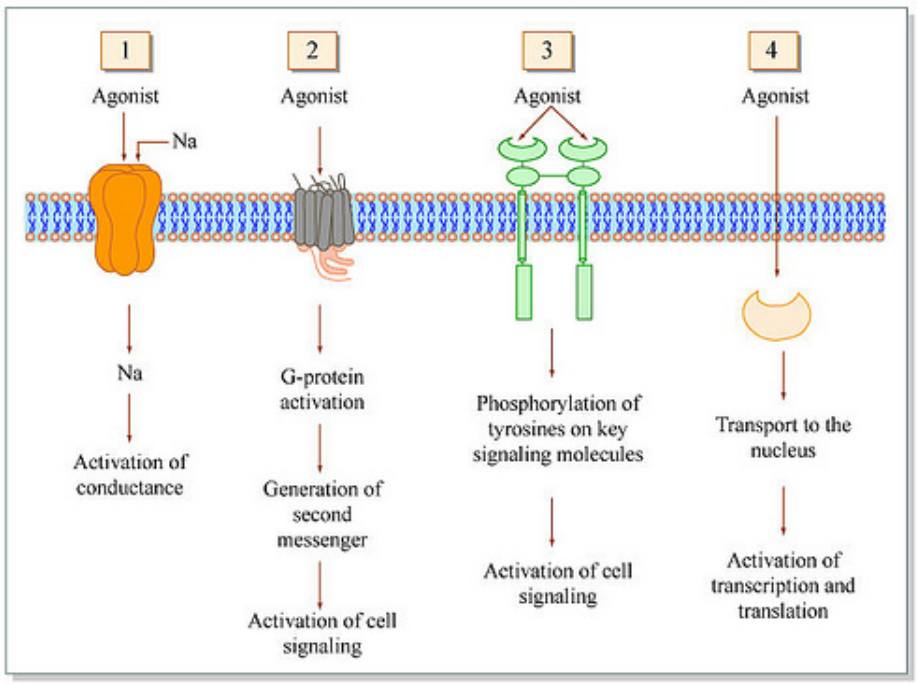

Figure 2.4: The four different types of receptors, with examples of signal transduction for each of it when specific agonist binds the binding site. Figure from *http://www.mc.uky.edu/* (n.d.).

All membrane receptors possess the same basic structure, as we can see in Figure 2.5: they all have an extracellular domain, a transmembrane domain, cytoplasmic domain. Based on more specific structural and functions similarities, membrane receptors can be grouped mainly in three different classes: the ion channel-linked receptor, the first displayed in Figure 2.4, the G protein-coupled receptor, number 2 in Figure 2.4, and the enzyme-linked receptor, the third in Figure 2.4 (*http://en.wikipedia.org/wiki/* n.d.).

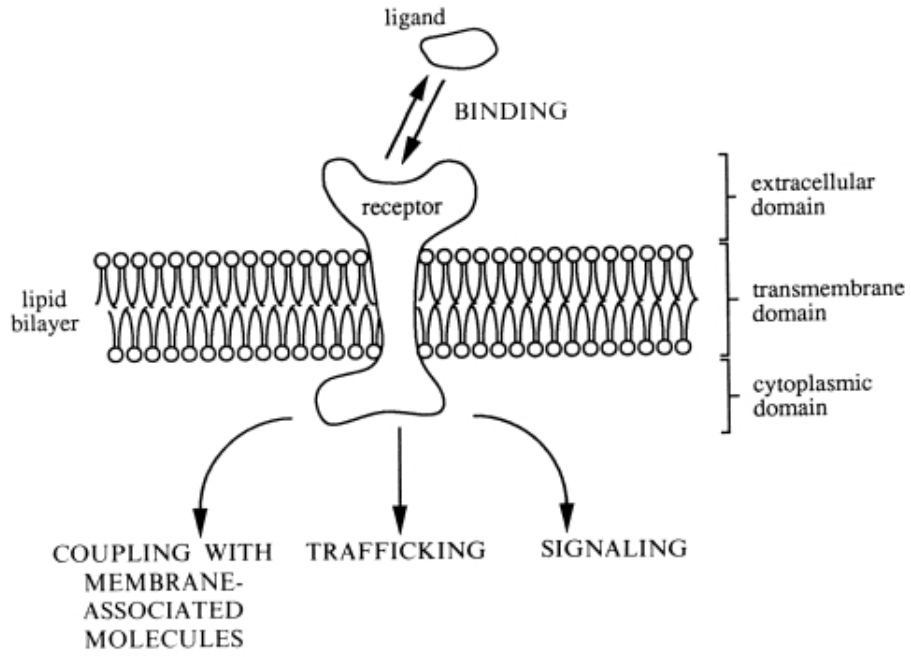

Figure 2.5: Schematic structure of cell receptors. Models for receptor binding, coupling with membrane-associated molecules, signaling, and trafficking. Figure from Lauffenburger & Linderman (1996)

To model a receptor, we need to take into account the level of complexity in receptor state (e.g., bound, unbound, coupled with other membrane-associated molecules) and location (e.g., cell, endosomes). Details of receptor/ligand binding kinetics at the cell surface, trafficking through the cell must be considered. The Figure 2.6 gives an example of different states the receptor can be found in and of the different locations. Receptors and their ligands can be internalized and routed through intracellular compartment and eventually recycled, degraded or synthesized.

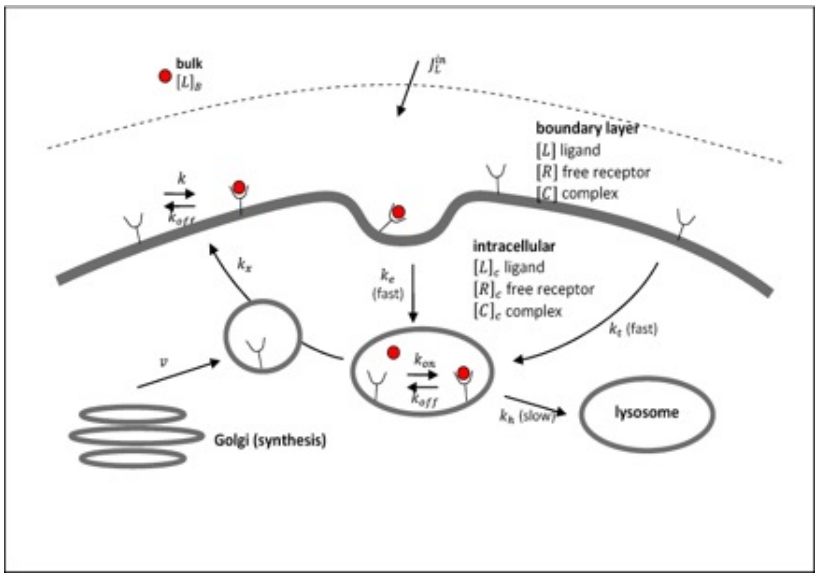

Figure 2.6: Different levels of complexity in receptor state and location. Figure from Alberts (2010)

3.1 Cell surface receptor binding models

The simplest model we can assume is that of a monovalent ligand L binding to a monovalent receptor R, to form a complex C.

$$L + R \underset{k_r}{\overset{k_f}{\rightleftharpoons}} C$$

To describe the rate of change of the receptor/ligand complex we will use the *mass action kinetics* so that:

$$\frac{dC}{dt} = k_f RL - k_r C \tag{2.11}$$

where k_f is the association rate constant (M^{-1} time^{-1}) and k_r is the dissociation rate constant (time^{-1}). Assuming that the total surface receptor number R_T is constant and the total amount of ligand L_0 is unchanged, we

can apply the *conservation law* at all time:

$$R_T = R + C \tag{2.12}$$

$$L_0 = L + \Big(\frac{n}{N_{Av}}\Big)C \tag{2.13}$$

$$\frac{dC}{dt} = k_f(R_T - C)L_0 - k_r C \tag{2.14}$$

where N_{Av} is Avogadro's number and n is the concentration of the cell in the medium. With an initial condition of $C(t = 0) = C_0$, after a transient state, the complex reaches equilibrium with $\frac{dC}{dt} = 0$ and the number of receptor/ligand complex is:

$$C_{eq} = \frac{R_T \cdot L_0}{K_D + L_0} \tag{2.15}$$

where K_D is the equilibrium dissociation constant

$$K_D = \frac{k_r}{k_f} \tag{2.16}$$

This is a really simplified case of the binding. When the ligand concentration is not constant in time, we should consider *ligand depletion effects* and the complex rate of change is not linear anymore in the receptor/ligand complex number. The receptor occupancy at steady-state can be described in a form of an implicit equation. Using a dimensionless number of complexes, u, to represent the fraction of receptors occupied, a dimensionless time τ, that can be thought of as complex "turnover" number during time t, and a scaled cell density, η, defined as:

$$u = \frac{C}{R_T} \tag{2.17}$$

$$\tau = k_f \cdot t \tag{2.18}$$

$$\eta = \frac{nR_T}{N_{Av}L_0} \tag{2.19}$$

the fractional receptor occupancy at equilibrium is

$$u_{eq} = \frac{L}{K_D + L} = \frac{L_0[1 - \eta u_{eq}]}{K_D + L_0[1 - \eta u_{eq}]} \tag{2.20}$$

This is just an example of different dynamics affecting receptor binding. Other types of interaction that can take place on the cell membrane can be *non-specific binding*, when the unbound receptor is subtracted from the pool by binding a non-specific substance so that it cannot bind the ligand anymore, *cooperativity*, when KD appear to vary with the extent of receptor occupancy by ligand, *multiple receptor states*, as *receptor subpopulations* may be recognized because of *molecularly distinct receptor types* or a *conversion* between different forms of molecular type which finally affect the binding properties, *ternary complex* models, when the receptor interacts with some membrane-associated proteins, such as G-proteins, coated pit adaptors, and *receptor aggregation*. Receptor/ligand complexes can accumulate in localized membrane regions, called *coated pit* or *smooth pit*, structures that selectively trap molecules on the cell surface in the process named *endocytosis*. Coated pits invaginate and pinch off to form intracellular vesicles in the cytoplasm. Their destination is established in a process called *endosomal sorting*. Due to *internalization* and due to the *synthesis* of new receptors, the number and distribution on the cell surface varies. These processes are considered in the *dynamic trafficking events*. Mathematical models for receptor/ligand trafficking can be divided into two levels: models describing the kinetics of receptor/ligant movement through whole cells, called "Whole-cell kinetic models", where we quantify the rate constants for the trafficking processes of

the model, and models describing specific mechanisms involved in the endocytic cycle, called "Mechanistic models", where we evaluate biochemical and biophysical properties of the receptors, ligands and other components of the endocytic cycle. Since trafficking processes alter the number of receptors in the cell membrane and the amount of ligand in solution, receptor/ligand binding will never be at chemical equilibrium. To give an example of a base whole-cell kinetic model for endocytosis, we will assume a simple bimolecular, non-cooperative receptor/ligand binding. The receptor, R_S, and the complex on the cell surface, C_S, can be internalized in the endosome with rate constants k_{eR} and k_{eC} respectively, where we will refer as R_{Ti} the total number of free plus bound receptors in endosomes and as $L_i^{\#}$ the amount of intracellular ligand. The receptor R_S is synthesized at a rate V_S. The receptors and the ligands in endosomes can be transported back to the cell surface at a rate k_{rec} by vesicles, with constants (1-f_R) and (1-f_L) respectively denoting the fraction of endocytosed receptors and of ligand toward the surface to be recycled. Another direction the vesicles can be routed, at a rate k_{deg}, is the lysosome, where they are degraded in a fractional amount denoted as f_R and f_L respectively. To complete the assumption we must say that the ligand is uptaken at rate $k_{fp} \cdot N_{Av} \cdot L$ and that the total amount of ligand L in the medium is constant. The kinetic balance equations are:

$$\frac{dR_S}{dt} = -k_f L R_S + k_r C_S - k_{eR} R_S + k_{rec}(1 - f_R) R_{Ti} + V_S \tag{2.21}$$

$$\frac{dC_S}{dt} = k_f L R_S - k_r C_S - k_{eC} C_S \tag{2.22}$$

$$\frac{dR_{Ti}}{dt} = k_{eR} R_S + k_{eC} C_S - [k_{rec}(1 - f_R) + k_{deg} f_R] R_{Ti} \tag{2.23}$$

$$\frac{dL_i^{\#}}{dt} = k_{eC} C_S - [k_{rec}(1 - f_L) + k_{deg} f_L] L_i^{\#} + k_{fP} N_{Av} L \tag{2.24}$$

This model describes the general trafficking effects and can be analyzed for specific experimental system.

Chapter 3

Mathematical modeling for VIP receptor: novel model

Having recognized the importance of the role of VIP and its receptor $VPAC_2$ in the circadian mammalian system and having explored mathematical modeling for receptors, we found it necessary to integrate the ligand-receptor dynamics in the mammalian model. We first want to model $VIP - VPAC_2$ role in the communication among neurons and we want to investigate the effect of adding the neurotransmitter in a network of cells. We start from the Mirsky et al. model for the single cell neuron, and we will generate a pool of 16 cells, equally spaced distributed on a square grid of a side size of 4 cells, to explore the coupling mechanism. Mirsky core model was modified with To *et al.*'s coupling equations, shown in Figure 3.1.

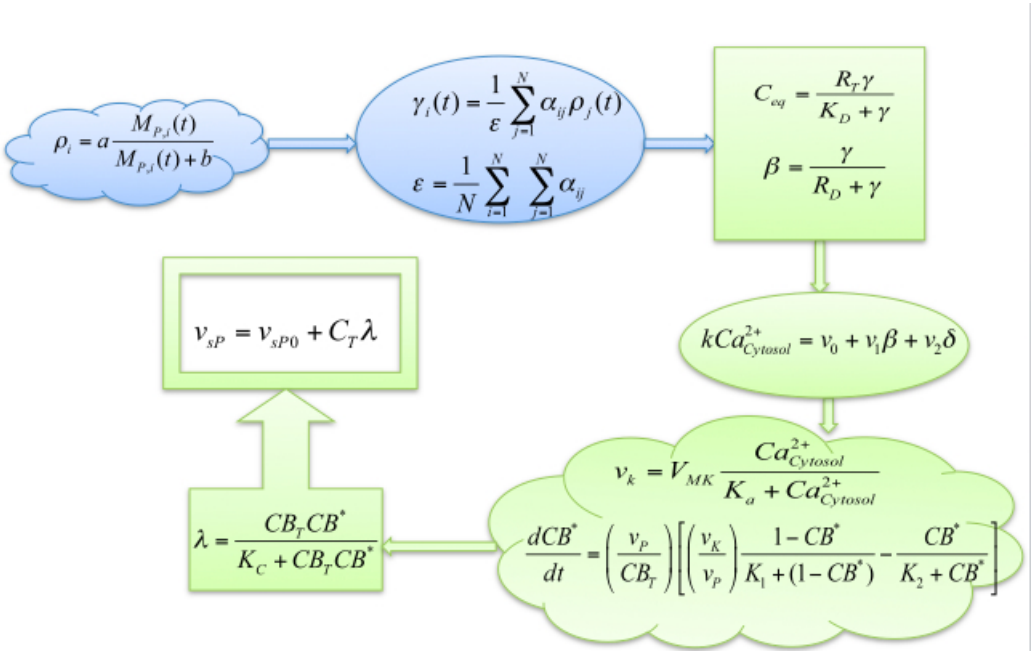

Figure 3.1: Model of To's coupling VIP release and cascade.

The coupling mechanism can be summarized as:

- the amount of extracellular VIP release is circadian and proportional with a *Michaelis-Menten* term to *Per2* mRNA and augmented by light. VIP dose seen by each cell of the grid is a weighted amount by the distance from the cells in the grid.

- Intracellular VIP cascade includes cytosolic Calcium release which leads to CREB phosphorylation and it finally affects *Per* transcription

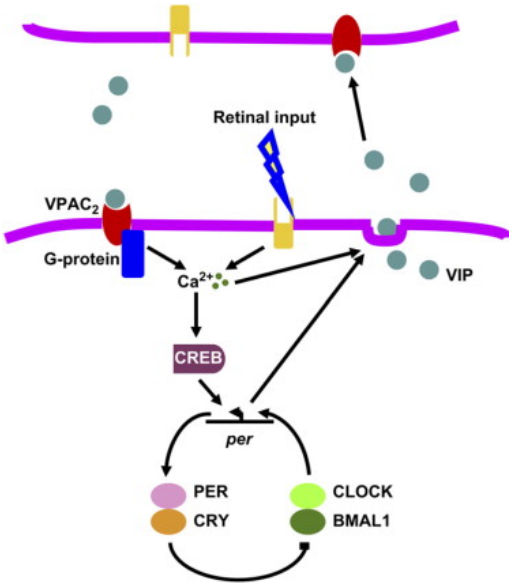

Figure 3.2: Schematic of the mechanism modeled to generate and synchronize circadian rhythms in the SCN. Figure from To et al. (2007).

We modified the receptor dynamics in this model starting from a simple hypothesis of the model to see if we could capture the oscillation of the system, achieve the synchrony of the neurons in the network without losing the phase relationships between different components. The $VPAC_2$ receptor is still modeled as a monovalent ligand that binds reversibly to the VIP protein but its total amount in the cell surface is not assumed to be constant anymore. VIP is assumed to be produced at basic rate v0 and proportional through a *Michaelis-Menten* term to PER2 protein amount.

An additional state became necessary, to model time variation of the $VIP - VPAC_2$ complex formation, instead of the assumption of its equilibrium. The equilibrium concentration of the complex, C_{eq}, or the ratio β of the complex density to the total receptor density (R_T) of To *et al.*'s coupling dynamic model, were changed with these new assumptions.

Modifying the Mirsky *et al.* model, we needed to estimate the parameters we

integrated the model with. Even if a parameter set for To *et al.*'s coupling cascaded had already been estimated for that model, we decided to recalculate all the parameter values in the coupling model because of the altered general assumptions.

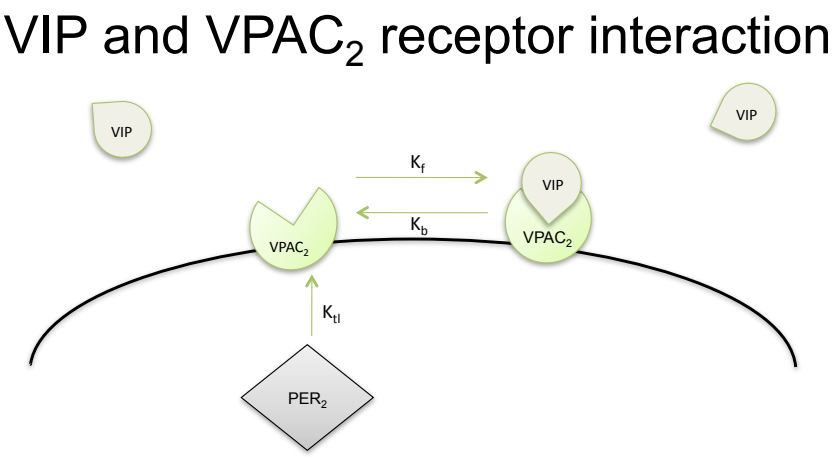

$$VPAC_2 = v_0 + v_1 * \frac{PER_2}{K_M + PER_2}$$

$$\frac{dVIP\_VPAC_2}{dt} = K_f * VPAC_2 * VIP - K_b * VIP\_VPAC_2$$

Figure 3.3: Schematic of the modified mechanism modeled to generate and synchronize circadian rhythms in the SCN. Model n.1.

The model with the coupling mechanism we started from was composed of:

- 22 states
- 6 algebraic equations
- 132 fixed parameters
- 19 estimated parameter from To et al.'s coupling cascade

We added in a first simple model (model 1):

- 1 state
- 1 algeabric equation
- 5 parameters

Resulting in a model of:

- 23 states
- 7 algebraic equations
- 132 fixed parameters
- 24 estimated parameters of the new coupling cascade

The complete matlab code of the model is in Appendix (*VPACcoupled_mm.m*). To find the optimum parameter values we ran the model for the single cell to find random initial condions for each of the 16 cells to oscillate (function *SingleCellAutoModel.m* in Appendix). We used a Genetic Algorithm (GA) to search for the best parameters.
The idea of the Genetic Algorithms is: given a population of individual, the environmental pressure causes natural selection (survival of the fittest) and this causes a rise in the fitness of the population. Given an objective function to be optimized (minimization or maximization are specular treated), the algorithmic procedure randomly create solutions, i.e. elements of the function's domain, and apply the objective function as an abstract fitness measure.
Based on this fitness, some of the better candidates are chosen to seed the next generation by applying recombination and mutation to them. Recombination is an operator applied to two or more selected candidates (called "parents") and results one or more new candidates (the "children"). Mutation is also applied to one candidate, modifying a very small part of it, and creating one new candidate. Executing recombination and mutation leads to a set of new points (the "offspring") that compete, based on their fitness,

with the old ones for a place in the next generation. This process is then reiterated until a candidate with sufficient quality is found or a previously set computational limit is reached. Eiben & Smith (2008)

The genetic algorithm used in this thesis generates 100 arbitrarily parameter sets (the "parents"), by sampling the parameter space. We define the parameters space giving the lower bound and the upper bound for each parameter in the cost function. The GA arbitrarily selects two "parents", combines parameters and mutates them to obtain 100 new parameter sets. This is the way the GA generates the "children". It computes the cost function value for each "child" and it saves the best 10 parameter sets, where "best" is considered in terms of the lowest fitness measure. These 10 "children" are now parents and the GA generates a new generation of 100 "children" by mutating and combining the parameters. It keeps on generating children from parents and saves the top parameter set as the "fittest", iterating the process 100 times (Grosman & Lewin 2004). We made multiple runs of the algorithm because it looks for an optimum starting from the particular sampling of the parameter space it makes to generate the first generation of parents. This optimum of the algorithm is made up of mutations and combinations of the initial sampling so that it depends on the initial conditions, conceived as the initial randomly sampling of the space.

As cost function, we used the constraint that all the cells oscillate in-phase (see *Cla_cost_fun_peak.m* in Appendix). To measure how far the cells were to oscillate in the same phase we defined an index: the Synchronization Index (SI), equal to:

$$SI = \frac{\sum_{i=1}^{N} e^{j\theta_i}}{N} \tag{3.1}$$

where N is the number of neurons of the grid and θ_i is the phase of the i-th neuron when the steady-state is achieved. SI can assume a value between 0 and 1 where 0 is a totally out of phase system and when the synchrony is

achieved, SI is equal to 1.

Since this simple model could achieve the synchrony among neurons of the grid and display a correct phase relationship among different components, we decided to add details to the model to confer it with more biological significance.

We chose to apply the following changes:

- We modeled $VPAC_2$ mRNA, based on the observation that it oscillates with a circadian pattern (Shinohara et al. 1999), as proportional with a *Michaelis-Menten* form to the PER2 mRNA.

- $VPAC_2$ receptor is supposed to oscillate, based on the observation that its mRNA oscillates. It can form a complex with VIP or be degraded in the cell surface, without any formation of the complex.

- The complex can be internalized, modulating the total complex formation and VIP cascade effect.

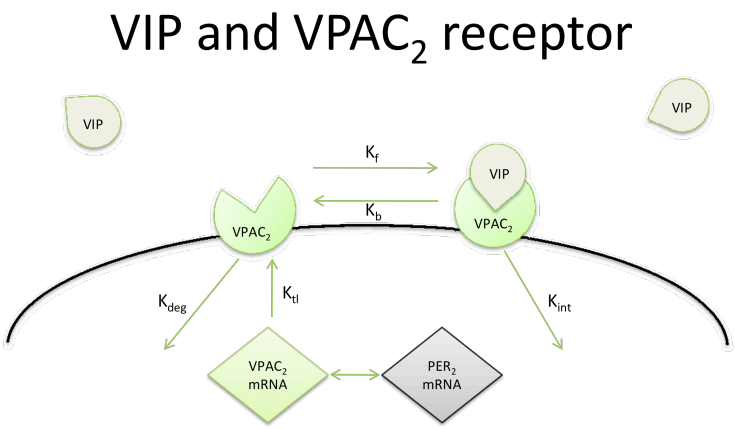

$$VPAC_2\_mRNA = v_0 + v_1 * \frac{PER_2\_mRNA}{K_M + PER_2\_mRNA}$$

$$\frac{dVPAC_2}{dt} = K_{tl} * VPAC_2\_mRNA - K_{deg} * VPAC_2 - K_f * VPAC_2 * VIP + K_b * VIP\_VPAC_2$$

$$\frac{dVIP\_VPAC_2}{dt} = K_f * VPAC_2 * VIP - K_b * VIP\_VPAC_2 - K_{int} * VIP\_VPAC_2$$

Figure 3.4: Schematic of the modified mechanism modeled to generate and synchronize circadian rhythms in the SCN. Model n.2.

Resulting a model (model 2) of:

- 24 states
- 7 algeabric equations
- 132 fixed parameters
- 26 estimated parameters of the new coupling cascade

The complete matlab code of the model is in Appendix (*VPACmRNA.m*). We ran again the GA to find an optimal parameter set.

Chapter 4

Results

Running the GA for the *model 1* we had 32 different parameter sets giving an SI equal to 1. The 32 parameter sets we found from different initial conditions with multiple runs of the GA are shown in Table 4.1:

This model showed that we could achieve synchrony in a network of single neurons by adding receptor dynamics. Since this model was not descriptive enough and we considered the results less significant with respect to the second model. So we focus here solely on the second model, *model 2*. We focus our attention on the more detailed model and the Table 4.2 that follows shows the 27 parameter sets we had as optimum, running the GA multiple times

	par.set #1	par.set #2	par.set #3	par.set #4	par.set #5	par.set #6	par.set #7	par.set #8
k	49,448	6,347	43,829	6,347	9,548	61,797	61,797	49,448
v0	0,799	1,931	0,799	1,931	0,648	2,414	2,414	2,165
v1	3,807	0,622	0,622	0,622	0,622	12,768	12,768	12,768
vP	6,675	8,186	8,186	8,186	5,987	4,164	4,164	7,407
VMK	16,019	18,873	6,228	18,873	10,818	4,140	4,140	18,873
Ka	6,041	2,818	5,313	2,818	4,630	2,818	2,818	3,988
K_1	0,639	0,422	0,093	0,422	0,808	0,139	0,139	0,901
K_2	0,049	0,242	0,093	0,242	0,422	0,422	0,422	0,139
CBT	5,465	1,055	1,432	1,055	7,579	3,198	3,198	5,465
KD	7,858	0,807	0,807	0,807	2,109	9,638	9,638	1,214
a	135,292	35,449	119,918	35,449	79,163	207,364	207,364	79,163
b	7,769	9,154	4,099	9,154	10,627	3,021	3,021	7,769
vs2P1	226,658	197,502	170,113	197,502	290,731	445,606	445,606	290,731
vs2P2	114,879	47,501	78,041	47,501	57,051	176,076	176,076	101,824
KA2P1	4,028	9,364	4,966	9,364	4,966	7,028	7,028	7,028
KA2P2	0,269	0,269	0,142	0,269	2,908	1,635	1,635	1,424
na2_P1	0,528	0,528	2,050	0,528	2,623	3,885	3,885	1,510
na2_P2	1,603	4,858	5,640	4,858	2,175	3,433	3,433	5,640
naCB	6,304	5,624	7,799	5,624	4,385	3,291	3,291	5,624
kbVIP_VPAC2	2,207	1,164	4,443	1,164	6,810	5,553	5,553	6,810
KMVPAC2	10,061	13,127	18,509	13,127	22,700	18,509	18,509	13,127
v0MVPAC	5,251	0,760	5,251	0,760	2,450	2,450	2,450	5,924
v1MVPAC	4,980	0,300	1,164	0,300	3,938	0,570	0,570	1,837
	par.set #9	par.set #10	par.set #11	par.set #12	par.set #13	par.set #14	par.set #15	par.set #16
k	49,448	6,347	43,829	6,347	24,557	61,797	61,797	49,448
v0	0,799	1,931	0,648	1,931	2,414	1,506	0,248	2,165
v1	3,807	0,622	0,622	0,622	8,160	8,160	0,622	10,320
vP	6,675	8,186	8,186	8,186	6,675	4,164	4,734	7,407
VMK	16,019	18,873	6,228	18,873	16,019	4,140	40,310	18,873
Ka	6,041	2,818	5,313	2,818	4,630	2,818	6,815	10,446
K_1	0,639	0,422	0,093	0,422	1,000	0,139	1,000	0,901
K_2	0,049	0,242	0,093	0,242	0,422	0,422	0,358	0,189
CBT	5,465	1,055	1,432	1,055	7,579	3,198	0,701	5,465
KD	7,858	0,807	0,807	0,807	0,807	7,858	2,600	1,214
a	135,292	35,449	119,918	35,449	79,163	207,364	17,364	35,449
b	7,769	9,154	3,021	9,154	13,866	3,021	2,008	2,008
vs2P1	226,658	197,502	76,176	197,502	226,658	403,186	363,335	290,731
vs2P2	114,879	47,501	78,041	47,501	67,218	176,076	176,076	101,824
KA2P1	4,028	9,364	0,811	9,364	4,966	7,028	18,409	7,028
KA2P2	0,269	0,269	0,142	0,269	2,908	1,635	0,142	1,424
na2_P1	0,528	0,528	2,050	0,528	2,623	3,885	6,933	1,510
na2_P2	1,603	4,858	5,640	4,858	8,302	3,433	3,433	5,640
naCB	6,304	5,624	7,799	5,624	4,385	3,291	3,291	5,624
kbVIP_VPAC2	2,207	1,164	4,443	1,164	2,207	5,553	6,810	6,810
KMVPAC2	10,061	13,127	18,509	13,127	2,860	18,509	8,666	13,127
v0MVPAC	5,251	0,760	5,251	0,760	0,400	2,450	0,760	5,924
v1MVPAC	4,980	0,300	1,164	0,300	6,162	0,300	5,553	1,490
	par.set #17	par.set #18	par.set #19	par.set #20	par.set #21	par.set #22	par.set #23	par.set #24
k	61,797	75,790	12,956	3,339	38,551	38,551	20,446	61,797
v0	2,165	1,130	0,130	1,712	0,130	1,312	0,130	0,648
v1	6,254	7,178	6,254	11,506	10,320	6,254	9,207	14,111
vP	5,987	7,407	4,734	7,407	5,341	1,400	6,675	6,675
VMK	44,731	49,438	16,019	6,228	6,228	36,157	18,873	21,912
Ka	3,988	6,815	7,640	3,988	0,875	10,446	6,815	10,446
K_1	0,808	0,808	1,000	0,139	0,242	0,562	0,242	1,000
K_2	0,358	0,808	0,298	0,298	0,490	0,189	0,562	0,298
CBT	4,844	1,432	7,579	4,261	3,198	1,833	3,713	3,198
KD	2,109	2,109	4,902	2,109	8,720	8,720	2,600	4,272
a	45,375	35,449	169,079	135,292	9,135	187,623	55,941	26,124
b	9,154	13,866	7,769	13,866	23,978	13,866	15,644	3,021
vs2P1	97,507	56,138	257,693	226,658	56,138	257,693	144,384	120,213
vs2P2	176,076	176,076	176,076	128,775	22,182	30,100	143,567	57,052
KA2P1	3,147	3,147	9,364	4,966	15,010	4,966	8,159	10,646
KA2P2	3,214	1,227	2,621	2,351	0,549	1,424	1,859	0,867
na2_P1	2,050	1,510	0,528	0,528	0,528	10,848	0,528	1,510
na2_P2	2,785	3,433	1,603	12,725	1,603	4,858	2,175	2,785
naCB	6,304	4,985	2,793	2,793	1,886	6,304	4,985	3,291
kbVIP_VPAC2	4,443	3,464	4,443	3,018	4,443	5,553	4,443	5,553
KMVPAC2	11,546	10,061	3,881	8,666	20,539	16,602	4,967	20,539
v0MVPAC	0,760	1,987	1,144	8,216	4,619	3,466	0,760	5,924
v1MVPAC	2,600	4,981	1,837	6,162	6,162	6,162	0,570	4,443
	par.set #25	par.set #26	par.set #27	par.set #28	par.set #29	par.set #30	par.set #31	par.set #32
k	55,430	49,448	12,956	3,339	38,551	33,592	24,557	61,797
v0	2,165	0,373	0,373	1,712	0,130	2,165	0,130	0,648
v1	6,254	6,254	7,178	11,506	10,320	6,254	9,207	12,768
vP	8,186	7,407	4,734	7,407	5,341	1,031	8,186	6,675
VMK	28,590	32,255	16,019	6,228	6,228	49,438	16,019	21,912
Ka	10,446	5,313	9,452	3,988	0,875	6,041	6,815	6,041
K_1	0,808	0,808	1,000	0,139	0,242	0,901	0,298	1,105
K_2	0,358	0,808	0,298	0,298	0,808	0,189	0,562	0,298
CBT	4,844	1,432	1,833	4,261	3,198	1,833	3,713	3,198
KD	2,109	2,109	7,049	2,109	8,720	3,123	2,600	4,272
a	79,163	35,449	207,364	135,292	9,135	119,918	55,941	26,124
b	7,769	13,866	7,769	13,866	23,978	10,627	15,644	7,769
vs2P1	120,213	97,507	257,693	226,658	144,384	144,384	144,384	97,507
vs2P2	176,076	114,879	128,775	128,775	22,182	30,100	143,567	38,529
KA2P1	3,147	1,542	16,657	4,966	15,010	4,028	9,364	10,646
KA2P2	3,214	1,227	0,867	2,351	0,549	1,424	1,859	0,703
na2_P1	1,510	1,510	0,528	0,528	0,528	1,510	0,528	0,528
na2_P2	2,785	3,433	1,603	12,725	1,603	4,858	2,175	9,307
naCB	7,029	4,385	2,793	2,793	1,886	2,793	4,985	8,620
kbVIP_VPAC2	1,837	2,207	4,443	3,018	4,443	5,553	4,443	3,018
KMVPAC2	22,700	3,881	1,901	3,881	20,539	13,127	4,967	8,666

Figure 4.1: The 32 parameter sets found running the GA for the simplest model.

	par.set #1	par.set #2	par.set #3	par.set #4	par.set #5	par.set #6	par.set #7	par.set #8	par.set #9
k	14,476	136,219	96,770	151,100	1,669	14,476	85,181	14,476	14,476
v0	5,901	3,327	1,132	0,565	0,565	0,307	4,774	4,261	5,901
v1	11,928	18,017	18,017	25,362	11,928	1,466	2,695	22,759	11,928
vP	0,850	9,201	3,991	9,201	16,321	3,131	11,785	11,785	0,850
VMK	79,736	29,635	71,170	88,855	5,135	14,028	55,563	79,736	88,855
Ka	13,338	5,093	16,848	7,506	13,338	11,740	1,995	11,740	13,338
K_1	0,314	1,083	0,423	0,662	0,211	0,211	0,794	0,539	0,314
K_2	0,115	0,024	0,662	0,115	0,115	0,024	0,423	0,423	0,115
CBT	7,080	4,084	2,377	7,080	7,080	1,600	10,695	9,414	8,211
KD	6,925	9,448	8,147	5,777	13,875	3,686	8,147	1,841	5,777
a	4,568	148,999	4,568	4,568	101,106	175,287	101,106	39,607	4,568
b	20,269	34,518	4,580	43,096	17,229	47,803	2,491	38,673	20,269
vs2P1	170,435	436,808	320,186	9,815	170,435	641,493	217,267	217,267	267,119
vs2P2	224,817	283,988	224,817	172,600	253,478	126,518	351,037	351,037	224,817
KA2P1	8,976	13,228	11,035	0,405	26,502	11,035	29,691	33,087	8,976
KA2P2	6,407	0,071	1,567	2,309	1,229	1,229	4,627	3,150	6,407
na2_P1	4,586	15,308	10,134	11,752	3,402	15,308	0,264	0,264	4,586
na2_P2	18,319	3,611	22,871	2,431	3,611	0,280	9,143	1,322	18,319
naCB	9,688	7,287	17,185	8,450	2,446	0,895	3,297	2,446	9,688
kbVIP_VPAC2	6,675	3,320	12,240	5,756	4,082	7,654	2,605	0,150	6,675
KMVPAC2	45,256	19,188	6,441	16,311	40,799	4,336	40,799	22,251	16,311
v0MVPAC	10,205	13,071	13,071	2,576	4,427	5,443	4,427	6,524	10,205
v1MVPAC	8,695	4,893	12,240	0,707	4,893	2,605	7,654	0,150	8,695
T1vpac2	1,675	2,257	4,241	3,538	1,675	7,536	6,633	5,785	11,766
degVPAC2T	0,050	3,268	2,898	0,050	0,868	4,080	2,225	2,898	1,361
KintVIP_VPAC2	0,434	0,644	0,644	4,526	0,644	1,919	0,050	1,107	0,434

	par.set #10	par.set #11	par.set #12	par.set #13	par.set #14	par.set #15	par.set #16	par.set #17	par.set #18
k	136,219	96,770	151,100	64,066	85,181	21,506	74,294	151,100	64,066
v0	3,327	1,774	0,065	0,565	0,307	4,774	2,127	2,502	2,127
v1	18,017	18,017	8,459	20,314	1,466	28,133	28,133	25,362	11,928
vP	9,201	5,882	9,201	16,321	3,131	11,785	8,025	9,201	14,714
VMK	29,635	71,170	88,855	14,028	63,123	79,736	41,790	41,790	55,563
Ka	5,093	13,338	5,093	13,338	11,740	11,740	6,262	13,338	15,038
K_1	1,083	0,423	0,423	1,411	0,024	0,423	1,083	1,083	0,314
K_2	0,024	0,662	0,115	0,115	0,024	0,794	0,662	0,024	0,934
CBT	4,084	2,377	9,414	7,080	1,600	9,414	10,695	3,204	3,204
KD	9,448	8,147	6,925	13,875	3,686	12,306	6,925	12,306	9,448
a	148,999	4,568	4,568	21,540	175,287	39,607	233,057	148,999	21,540
b	34,518	4,580	47,803	17,229	47,803	34,518	6,804	30,615	30,615
vs2P1	436,808	267,119	9,815	170,435	800,897	217,267	46,288	320,186	718,706
vs2P2	283,988	224,817	224,817	253,478	224,817	224,817	316,465	49,962	67,345
KA2P1	13,228	11,035	0,405	26,502	11,035	33,087	18,046	0,406	36,701
KA2P2	0,071	1,567	2,309	1,229	1,229	2,717	6,407	0,071	2,309
na2_P1	15,308	10,134	11,752	5,846	3,402	0,264	0,264	10,135	1,245
na2_P2	3,611	22,871	2,431	1,322	0,280	3,611	7,628	2,431	4,867
naCB	7,287	17,185	8,450	2,446	0,895	2,446	3,297	3,297	5,167
kbVIP_VPAC2	3,320	12,240	5,756	4,893	7,654	0,150	0,707	1,932	1,932
KMVPAC2	19,188	6,441	6,441	45,256	4,336	22,251	40,799	16,311	16,311
v0MVPAC	13,071	13,071	2,576	6,524	5,443	6,524	6,524	10,205	5,443
v1MVPAC	4,893	12,240	6,675	4,082	4,082	2,605	5,757	7,654	0,150
T1vpac2	2,257	4,241	3,538	7,536	5,785	5,785	2,257	2,878	11,766
degVPAC2T	3,268	2,225	0,050	0,868	4,080	2,551	1,107	1,107	2,898
KintVIP_VPAC2	0,644	0,644	4,080	1,631	2,225	1,361	1,919	1,631	2,225

	par.set #19	par.set #20	par.set #21	par.set #22	par.set #23	par.set #24	par.set #25	par.set #26	par.set #27
k	36,953	36,953	45,432	54,458	54,458	74,294	64,066	36,953	54,458
v0	2,127	2,127	3,327	2,502	2,502	0,840	1,443	1,443	0,065
v1	1,466	1,466	22,759	15,860	15,860	22,759	11,928	1,466	11,928
vP	13,204	13,204	9,201	14,714	14,714	10,453	14,714	13,204	16,321
VMK	48,462	48,462	55,563	24,105	24,105	1,089	55,563	48,462	55,563
Ka	18,775	18,775	7,506	6,262	6,262	6,262	10,240	18,775	18,775
K_1	0,314	0,314	0,024	0,423	0,423	1,083	0,314	0,115	0,539
K_2	0,423	0,423	0,423	0,211	0,211	0,211	0,934	0,423	0,211
CBT	10,695	10,695	3,204	15,055	15,055	10,695	3,204	10,695	9,414
KD	15,545	15,545	1,841	17,322	17,322	19,215	15,545	15,545	17,322
a	79,312	79,312	4,568	101,106	101,106	233,057	203,270	21,540	101,106
b	17,804	17,804	2,491	14,373	14,373	6,804	30,615	23,504	11,691
vs2P1	46,288	46,288	85,112	267,119	267,119	46,288	888,390	46,288	85,112
vs2P2	67,345	67,345	253,478	148,839	148,839	172,600	148,839	351,037	316,465
KA2P1	0,406	0,406	33,087	26,502	26,502	23,505	26,502	0,406	26,502
KA2P2	2,309	2,309	1,229	4,104	4,104	0,912	2,309	2,309	2,309
na2_P1	11,752	11,752	13,475	21,548	21,548	0,264	1,245	11,752	5,846
na2_P2	7,628	7,628	2,431	1,322	1,322	7,628	4,867	9,143	1,322
naCB	6,194	6,194	3,297	1,646	1,646	3,297	5,167	6,194	2,446
kbVIP_VPAC2	4,082	4,082	10,984	10,984	10,984	3,320	7,654	1,301	2,605
KMVPAC2	16,311	16,311	22,252	32,678	32,678	40,799	13,607	16,311	40,799
v0MVPAC	10,205	10,205	0,943	5,443	5,443	6,524	6,524	7,675	6,524
v1MVPAC	1,301	1,301	7,654	8,695	8,695	0,150	1,301	7,654	8,695
T1vpac2	5,785	5,785	5,785	8,496	8,496	3,538	6,633	7,536	8,496
degVPAC2T	1,107	1,107	1,631	4,080	4,080	1,107	3,661	1,631	4,080
KintVIP_VPAC2	1,919	1,919	2,898	1,631	1,631	1,919	2,898	1,631	1,631

Figure 4.2: The 27 parameter sets found running the GA for the more detailed model.

All the parameter set were producing a steady-state in the oscillation of the neurons in the grid with an $SI = 1$. We needed a new criterion to discriminate among different parameter sets and to judge whether they are good or not. We first checked the period of oscillation of the synchronized

cells at steady-state. We show in Figure 4.3 the distribution of the periods for every parameter set.

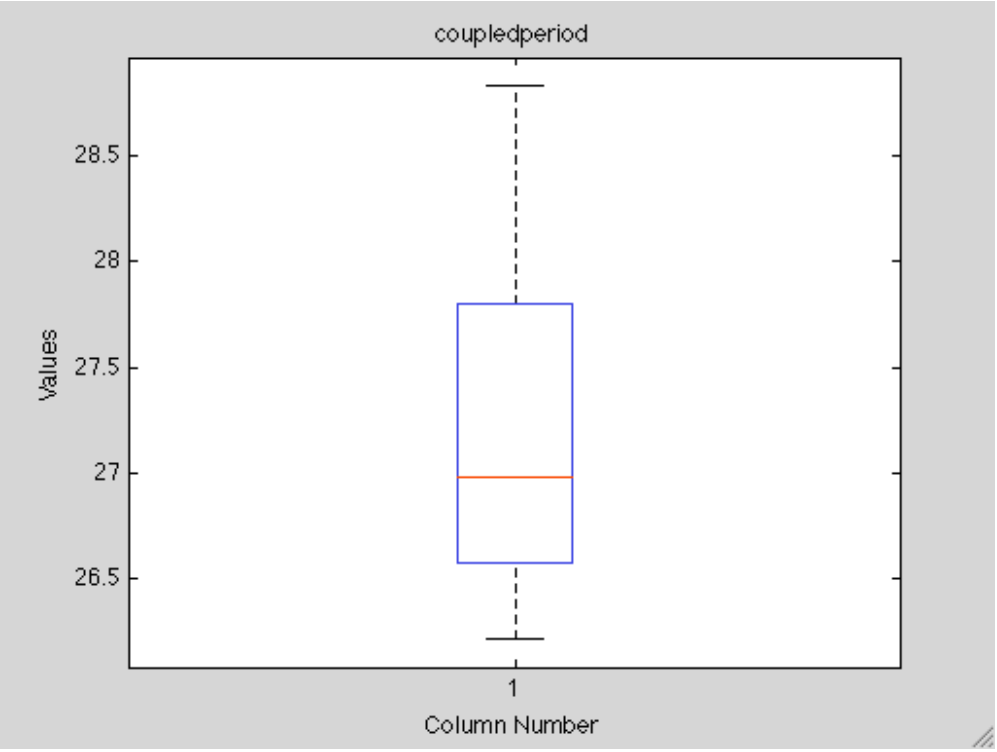

Figure 4.3: Boxplot of the distribution of the period for each parameter set.

The periods are all around a value of 27 hours that means that all the cells are synchronizing with almost the same period in all the parameters sets and the information about period length cannot be relevant to discriminate among different parameter sets.

Next, we tried to see if we could recognize a distribution of each parameter around a more stable value. We show the boxplot to analyze the distribution of values of each parameter. Since the numeric range changes significantly from one parameter to another, we decided to normalize each parameter by its mean value to have a better representation of the distribution. The boxplot of parameter set is shown in Figure 4.4:

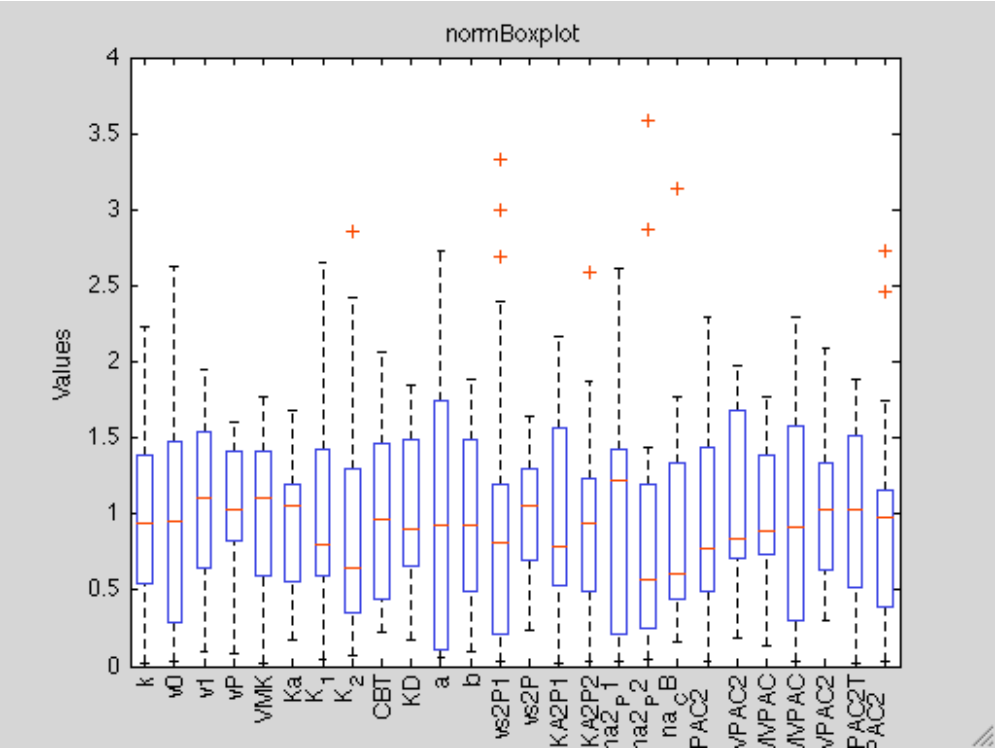

Figure 4.4: Boxplot of the distribution of the values for each parameter.

We can see how all the parameters are well distributed in their values and we cannot recognize a concentration around a specific value for each of them.
To select a parameter set as the best we decided to look at the parameter set that was giving us the smallest amplitude in the oscillation of the receptor pattern. We hypothesize that the receptor concentration oscillates and that it is circadian, based on the evidence that its mRNA expression is periodic, but we do not have any biological evidence that the protein also exhibits circadian oscillations. We suppose that maybe we are unable to capture a temporal varying pattern because of a too low signal/noise ratio and hence the $VPAC_2$ profile appears to be constant rather than oscillating. In other words, the amplitude is too small and we cannot detect it over the noise. The parameter set that corresponded to this characteristic was the 15^{th}. It

provides the temporal profiles of the main components shown in Figure 4.5:

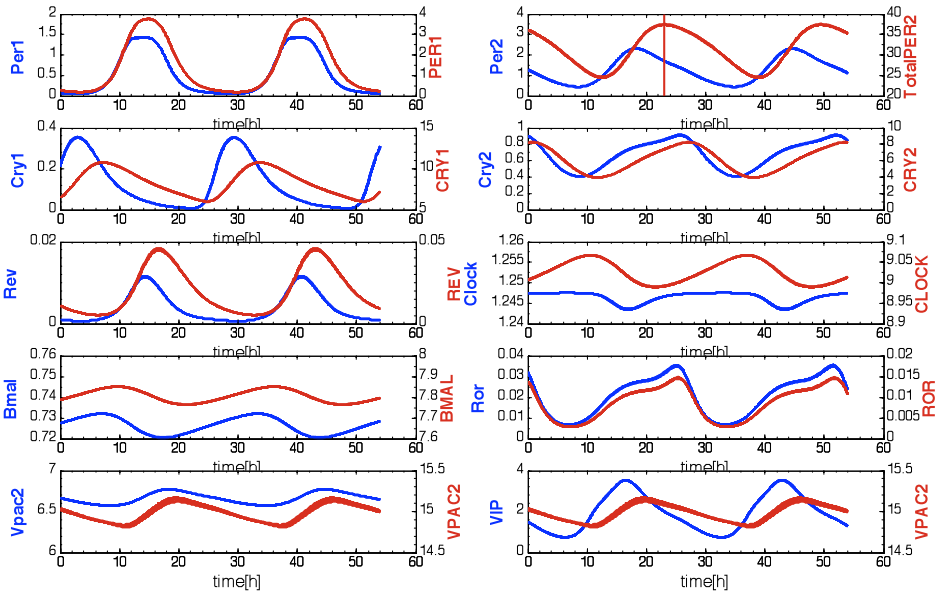

Figure 4.5: Temporal profiles of the main components for the parameter set that gives the minimum $VPAC_2$ amplitude.

and it predicts the temporal profiles for the VIP and the $VPAC_2$ shown in Figure 4.6. We are representing also the total PER2 protein profile because we take its peak as reference to fix the CT12.

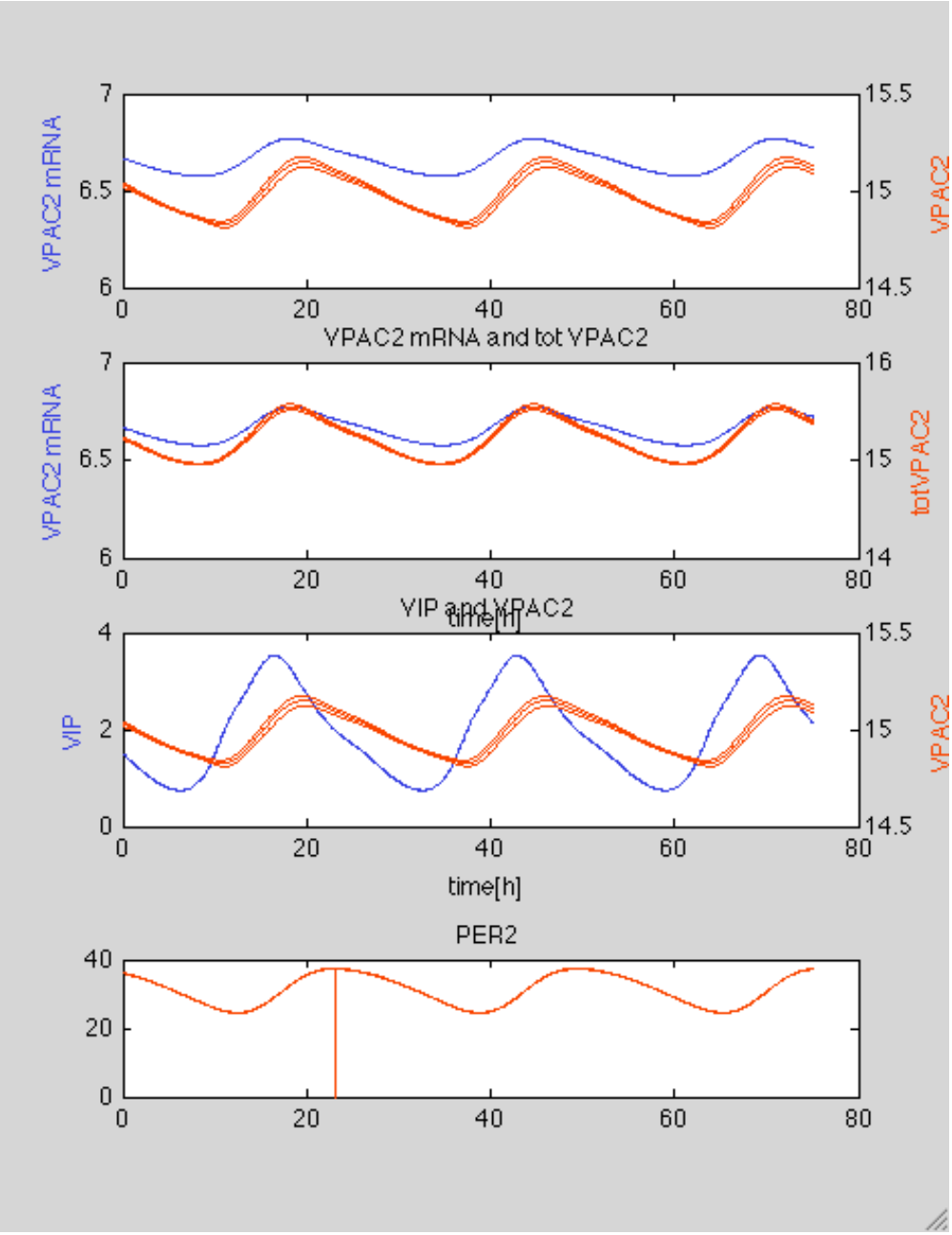

Figure 4.6: Temporal profiles of VIP and $VPAC_2$ for the parameter set that gives the minimum $VPAC_2$ amplitude.

To establish whether this parameter set was the best, we analyzed the phase shift among component, comparing our values to the same reference from

biological single cell data that Mirsky *et al.* used in their work (Mirsky 2010). The Table 4.7 represents the phases displayed by our model and the compared reference.

Phase shift	Reference	Model	Phase shift	Reference	Model
Period	23.7	26.4	Rev-ErbA mRNA → Per2 mRNA	~4 hours	3.9
Per1 mRNA → Per1 Protein	~5 hours	0.5	Rev-ErbA mRNA → Cry1 mRNA	~8 hours	11.4
Per2 mRNA → Per2 Protein	~5 hours	4.9	Rev-ErbA mRNA → Cry2 mRNA	~8 hours	14.3
Cry1 mRNA → Cry1 Protein	~5 hours	4.4	Rev-ErbA mRNA → RorC mRNA	~8 hours	10.1
Cry2 mRNA → Cry2 Protein	~5 hours	0.8	Rev-ErbA mRNA → Clk mRNA	~16hours	7.7
Rev-ErbA mRNA → Rev-ErbA Protein	~1 hour	2.3	Rev-ErbA mRNA → Bmal1 mRNA	~16hours	7.3
Clk mRNA → Clk Protein	~5 hours	4.0	VPAC2→ Per2 Protein	?	4.0
Bmal1 mRNA → Bmal1 Protein	~5 hours	2.7	tot VPAC2 →Per2 Protein	?	4.7
RorC mRNA → RorC Protein	~1 hour	0	VPAC mRNA →tot VPAC2	?	0.1
Rev-ErbA mRNA → Per1 mRNA	~4 hours	0.03	VIP→Per2 Protein	?	6.6

Figure 4.7: Comparison between phases of the reference and of the model for the minimun VIP amplitude parameter set.

We highlighted the major errors in the model prediction with rose colored cells to motivate our conclusion that the smallest $VPAC_2$ oscillation parameter set is not an appropriate one because it does not respect the predicted phase relationships among components.

As a new criterion to identify the best parameter set among the 27 found, we calculated the least square of the error as the distance of model predicted phases from the data reference phases. The best parameter set selected was the 3^{rd}.

The Figures 4.8 and 4.9 show the temporal profiles of the main components and the Table 4.10 provides the phase relationships.

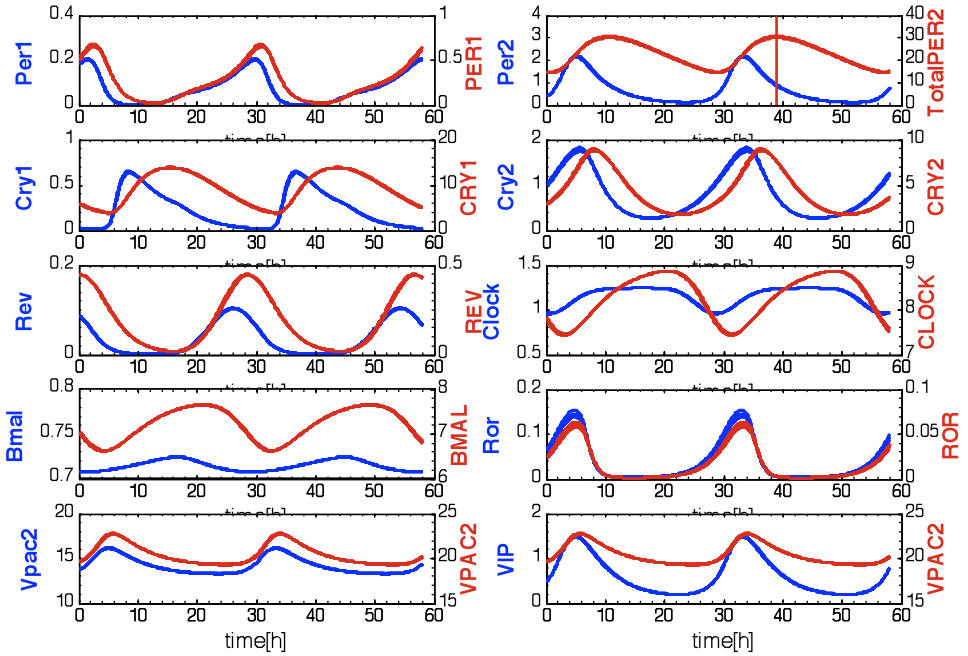

Figure 4.8: Temporal profiles of the main components for the parameter set that gives the minimum least square of the error.

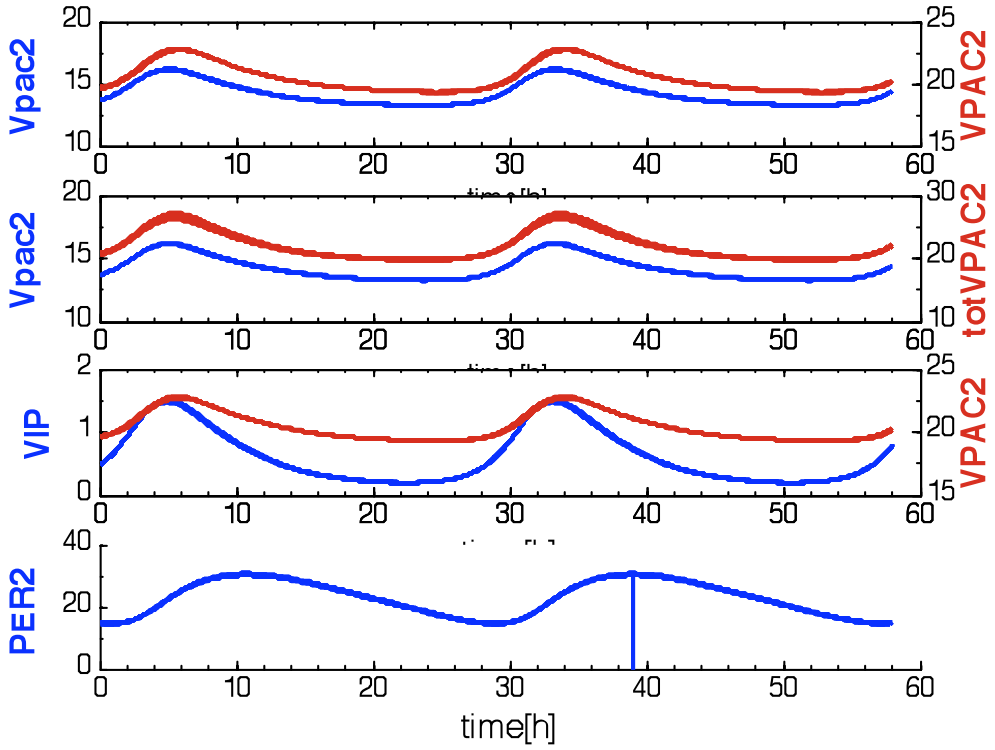

Figure 4.9: Temporal profiles of VIP and $VPAC_2$ for the parameter set that gives the minimum least square of the error.

Phase shift	Reference	Model	Phase shift	Reference	Model
Period	23.7	28.2	Rev-ErbA mRNA → Per2 mRNA	~4 hours	5.5
Per1 mRNA → Per1 Protein	~5 hours	1.0	Rev-ErbA mRNA → Cry1 mRNA	~8 hours	8.9
Per2 mRNA → Per2 Protein	~5 hours	5.6	Rev-ErbA mRNA → Cry2 mRNA	~8 hours	6.2
Cry1 mRNA → Cry1 Protein	~5 hours	7.0	Rev-ErbA mRNA → RorC mRNA	~8 hours	5.3
Cry2 mRNA → Cry2 Protein	~5 hours	2.4	Rev-ErbA mRNA → Clk mRNA	~16hours	16.7
Rev-ErbA mRNA → Rev-ErbA Protein	~1 hour	0.6	Rev-ErbA mRNA → Bmal1 mRNA	~16hours	17.0
Clk mRNA → Clk Protein	~5 hours	4.3	VPAC2→ Per2 Protein	?	4.8
Bmal1 mRNA → Bmal1 Protein	~5 hours	4.3	tot VPAC2 →Per2 Protein	?	5.2
RorC mRNA → RorC Protein	~1 hour	0.3	VPAC mRNA →tot VPAC2	?	0.4
Rev-ErbA mRNA → Per1 mRNA	~4 hours	2.0	VIP→Per2 Protein	?	5.7

Figure 4.10: Comparison between phases of the reference and of the model for the minimun VIP amplitude parameter set.

We decided to consider the parameter set that gave the best phase relationships as the most representative parameter set.

As further analysis we studied the responsiveness of the model to a 100 nM VIP pulse of 1hr duration, delivered at different circadian times. We constructed the Phase Response Curve (PRC) for all the parameter sets and we observed that the curves all had the same shape and were simply scaled in a range of values of magnitude of the shift. They were distributed but we could group them into three classes that we show in Figure 4.11:

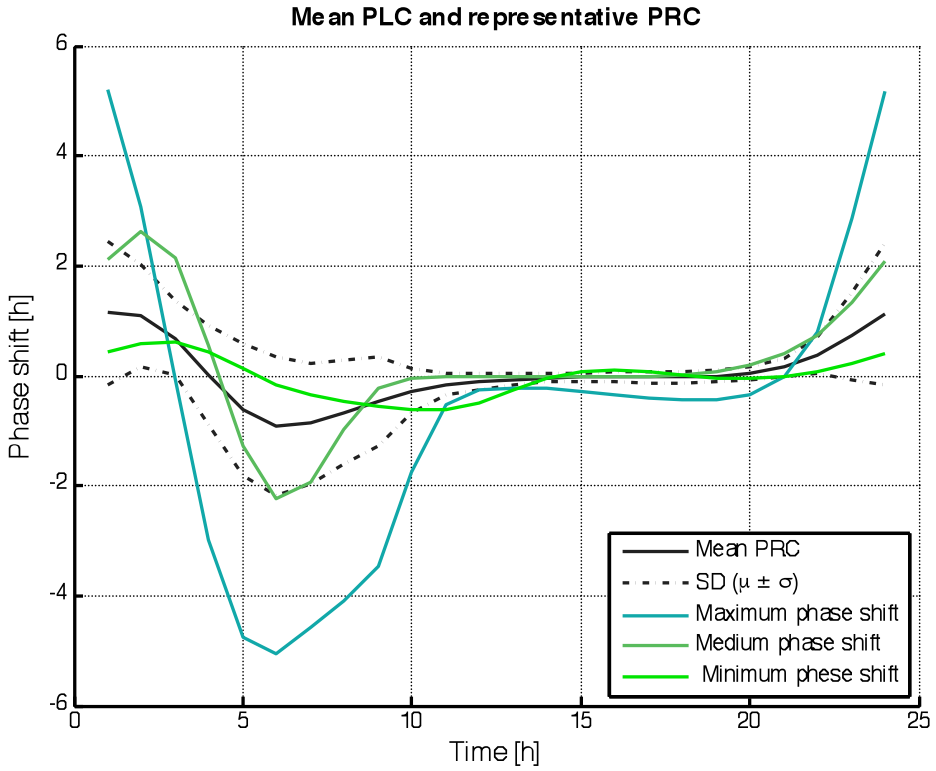

Figure 4.11: Average PRC and PRC for the three main classes.

We can say that all the parameter sets were giving a consistent PRC curve: the same parameter set that was giving the most positive shift at CT1 is the same as that which has the most negative at CT6. The PRC shape of our mammalian model is similar to the mouse PRC known from the literature. These observations confer more significance to our model. The PRC only differs in the dead zone around CT15 that is not supposed to be flat.

We continued our analysis using the parameter set that was giving the smallest least square. We decided to compare our new model behavior with the previous Mirsky *et al.* model integrated with To *et al.*'s coupling mechanism. We focused on the effect of the receptor-ligand dynamic of the new model on the synchrony, always estimated as a value of SI. We generated random

initial conditions for all the states of the model for the cells in the grid and we used these same values to run the time series of the model for each parameter set, tracking the SI temporal profile. We runned the old model with the same initial conditions for the states it has in common with the new model and tracked the SI profile for this model too. The Figure 4.12 shows the mean of the SI profiles of the 27 parameter sets and the SI profile of the old model.

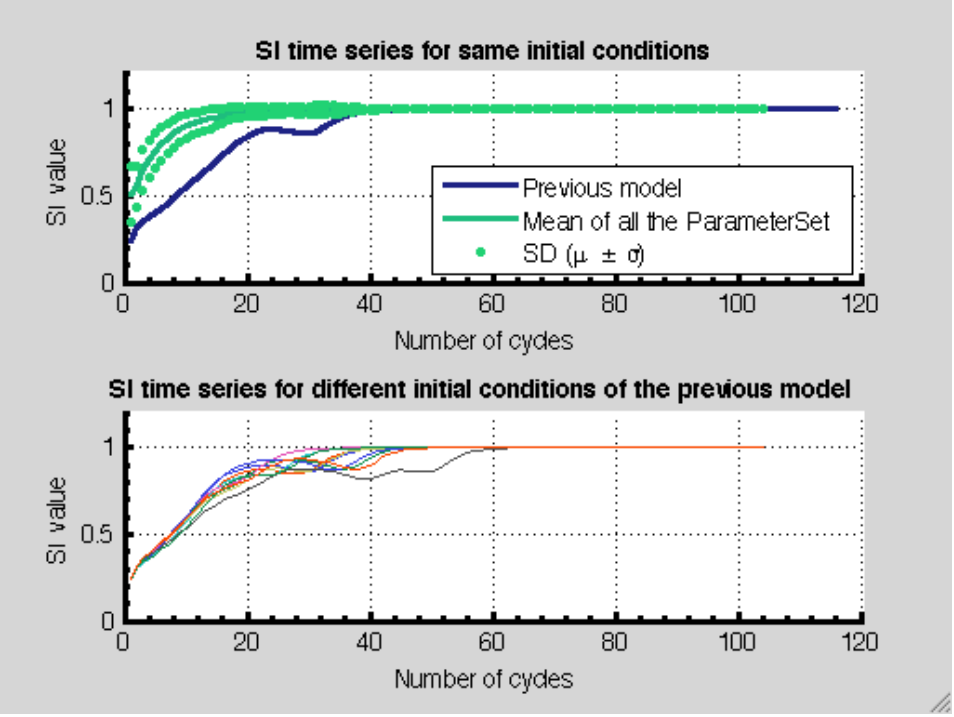

Figure 4.12: In the upper subplot: Mean and SD of the temporal profiles of the SI for all the parameter sets and for the previous model, with the same initial conditions. In the lower subplot: SI temporal profile for the previous model with 10 different initial conditions.

We can notice how adding explicit receptor dynamics could allow the model to reach faster a state in which the SI is next to 1, independently of the specific parameter set used for the new model. To make sure that the initial conditions were not some "unlucky" initial conditions for the old model, for

which it needed more time to synchronize, we generated 10 different random initial conditions for this model and we observed whether the SI profile was changing depending on the initial conditions. Since the SI temporal profiles were all similar we can confirm that the addition of the new receptor-ligand dynamic leads the system to achieve a faster synchrony. The $VPAC_2$ and VIP neurotransmitter role is supposed to make the neurons communicate and we consider it an important result that the addition of this mechanism to the model has the effect of making the cells rephase themselves on the same rhythm.

To quantify the time at which the synchrony was achieved for each parameter set we looked at how many cycles were necessary for the SI to reach the threshold value of 0.99.

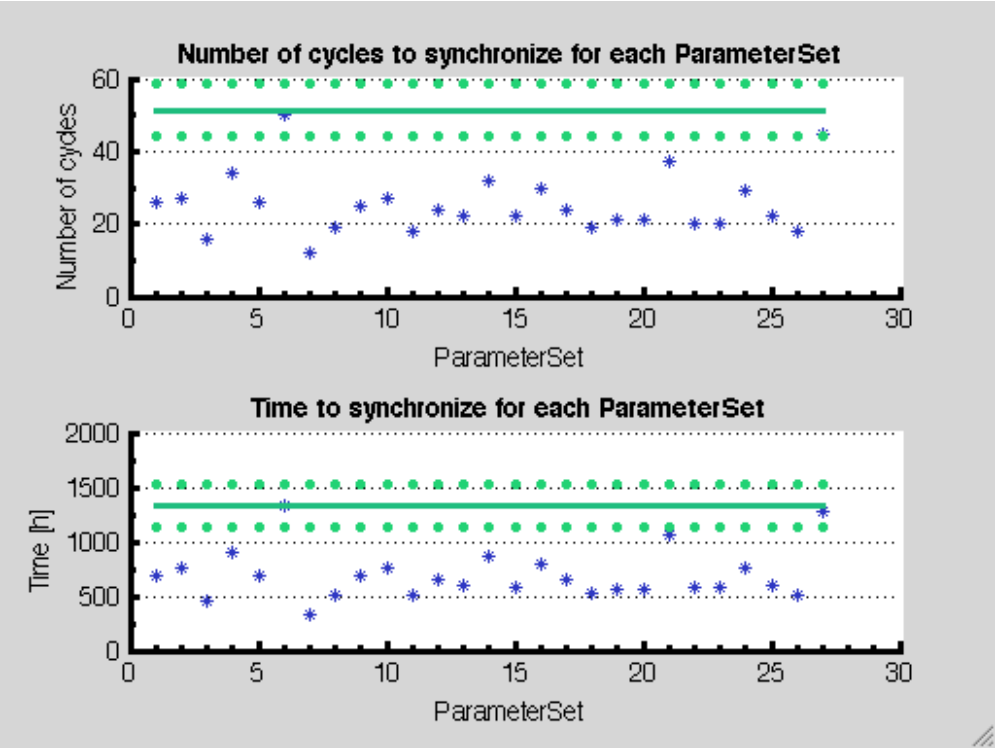

Figure 4.13: In the upper subplot: the blue stars are the number of cycles for the SI to reach the threshold value of 0.99 for each parameter set with the same initial condition, the green is the mean (line) and SD (dotted line) for 10 different initial conditions for the old model (green).

Every parameter set was giving different period lengths so we compared them in terms of hours for the SI to reach the threshold considering the corresponding amount of hours in a cycle for different parameter sets. We confirmed that the adding of the $VPAC_2$ leads to facilitate the synchrony of the neurons.

Chapter 5

Discussion and future work

We integrated the Mirsky *et al.* mammalian model with the $VIP - VPAC_2$ communication in a grid of 16 cells. We used hypotheses from the literature to develop the new model and to validate the parameter set against predictions from the literature. We found that the model can predict the synchrony among neurons to highlight the role of the $VIP - VPAC_2$ in the phase setting among neurons, resulting in synchrony in the oscillation. Unfortunately, we do not have any biological evidence to confirm the hypothesis we assumed on the $VPAC_2$ receptor oscillation and the model should be strengthened by providing biological evidence and data of $VPAC_2$ oscillation.

We found a wide range of parameters that lead the model to synchronize. This can be useful in the future if we decide to add detail to the model. We will be able to choose among a wide number of parameter sets to find an appropriate combination of parameters that will also allow the synchrony of the phases with the new details integrated in the model.

We should also work in order to find a more faithful phase relationship among components and maybe a fit of the model against biological data could identify a better parameters set in term of phase relationships.

Our model has been tested to see if it had a correct PRC and we found

that all the parameter sets were producing the same shape curve but scaled in amplitude. A consistent PRC could confer more reliability to our model. In future, the model should be modified to improve PRC shape: it shows a dead-zone (flat region) around CT15 that contrary to experimentally measured VIP PRC.

We then explored the SI time course for all the parameter sets and we found that the receptor helps the model to synchronize faster. As future work, we should integrate the VIP intercellular cascade to show a more detailed description of the mechanism of the cascade, such as parallel signaling through Ca^{2+} and cAMP and mechanistic form effect of CREB on *Per* transcription and phase relationship of VIP release.

Bibliography

Aderem, A. (2005), 'Systems biology: Its practice and challenges', *Cell* **121**(4), 511–513.

Alberts, B. (2010), *Essential cell biology*, Garland Science.

Aton, S., Colwell, C., Harmar, A., Waschek, J. & Herzog, E. (2005), 'Vasoactive intestinal polypeptide mediates circadian rhythmicity and synchrony in mammalian clock neurons.', *Nature neuroscience* **8**(4).
URL: *http://ukpmc.ac.uk/abstract/MED/15750589*

Aton, S., Huettner, J., Straume, M. & Herzog, E. (2006), 'Gaba and gi/o differentially control circadian rhythms and synchrony in clock neurons.', *Proceedings of the National Academy of Sciences of the United States of America* **103**(50).
URL: *http://ukpmc.ac.uk/abstract/MED/17138670*

Brown, T. & Piggins, H. (2007), 'Electrophysiology of the suprachiasmatic circadian clock.', *Prog Neurobiol* **82**(5), 229–255.

Cassman, M., Arkin, A., Doyle, F., Katagiri, F., Lauffenburger, D. & Stokes, C. (2007), *Systems Biology: International Research and Development*, 1 edn, Springer.

Ciarleglio, C., Gamble, K., Axley, J., Strauss, B., Cohen, J., Colwell, C. & McMahon, D. (2009), 'Population encoding by circadian clock neurons

organizes circadian behavior.', *The Journal of neuroscience : the official journal of the Society for Neuroscience* **29**(6), 1670–1676.

Colten, H. R. & Altevogt, B. M. (2006), *Sleep disorders and sleep deprivation: an unmet public health problem*, IOM of the National Academies press, Washington D.C.

Connor, J., Whitlock, G., Norton, R. & Jackson, R. (2001), 'The role of driver sleepiness in car crashes: a systematic review of epidemiological studies', *Accident Analysis Prevention* **33**(1), 31 – 41.
URL: *http://www.sciencedirect.com/science/article/B6V5S-418PNWR-4/2/69622ea336b30eee5f094b958a9937a3*

de Mairan, J. J. D. (1729), 'Observation botanique'.

Dragich, J., Loh, D., Wang, L., Vosko, A., Kudo, T., Nakamura, T., Odom, I., Tateyama, S., Hagopian, A., Waschek, J. & Colwell, C. (2010), 'The role of the neuropeptides pacap and vip in the photic regulation of gene expression in the suprachiasmatic nucleus', *European Journal of Neuroscience* **31**(5), 864–875.

Dunlap, J., Loros, J. & Decoursey, P. (2003), *Chronobiology: Biological timekeeping*, Sinauer Associates Inc.,U.S.

Edelstein-Keshet, L. (2005), *Mathematical Models in Biology*, Society for Industrial & Applied Mathematics.

Eiben, A. & Smith, J. (2008), *Introduction to Evolutionary Computing*, Springer.

Fall, C., Marland, E. & Wagner, J. (2002), *Computational Cell Biology*, Springer.

Gangwisch, J., Heymsfield, S., Boden-Albala, B., Buijs, R., Kreier, F., Pickering, T., Rundle, A., Zammit, G. & Malaspina, D. (2006), 'Short sleep duration as a risk factor for hypertension: analyses of the first national health and nutrition examination survey.', *Hypertension* **47**(5), 833–839.

Golombek, D. & Rosenstein, R. (2010), 'Physiology of circadian entrainment.', *Physiological reviews* **90**(3), 1063–1102.

Grosman, B. & Lewin, D. R. (2004), 'Adaptive genetic programming for steady-state process modeling', *Computers & Chemical Engineering* **28**(12), 2779–2790.
URL: *http://www.sciencedirect.com/science/article/B6TFT-4DMW22F-1/2/3e0d065d49ca47901dac832951154da0*

Hao, H., Zak, D., Sauter, T., Schwaber, J. & Ogunnaike, B. (2006), 'Modeling the vpac2-activated camp/pka signaling pathway: From receptor to circadian clock gene induction', *Biophysical Journal* **90**(5), 1560–1571.

Harmar, A. J., Marston, H. M., Shen, S., Spratt, C., West, K. M., Sheward, W. J., Morrison, C. F., Dorin, J. R., Piggins, H. D., Reubi, J.-C., Kelly, J. S., Maywood, E. S. & Hastings, M. H. (2002), 'The $vpac_2$ receptor is essential for circadian function in the mouse suprachiasmatic nuclei', *Cell* **109**(4), 497–508.
URL: *http://www.sciencedirect.com/science/article/B6WSN-45X0FCT-C/2/3ca0efa2b82e82d9ae5205384cd0feb9*

Hastings, M. H., Maywood, E. S. & O'Neill, J. S. (2008), 'Cellular circadian pacemaking and the role of cytosolic rhythms', *Current biology : CB* **18**(17), 805–815.
URL: *http://linkinghub.elsevier.com/retrieve/pii/S0960982208008889*

Hastings, M., O'Neill, J. S. & Maywood, E. S. (2007), 'Circadian clocks: regu-

lators of endocrine and metabolic rhythms', *J Endocrinol* **195**(2), 187–198.
URL: *http://joe.endocrinology-journals.org/cgi/content/abstract/195/2/187*

Herzog, E. (2007), 'Neurons and networks in daily rhythms', *Nature Reviews Neuroscience* **8**(10), 790–802.

http://en.wikipedia.org/wiki/ (n.d.), http://en.wikipedia.org/wiki/Transmembrane_receptor.

http://universe-review.ca/ (n.d.), http://universe-review.ca/I10-67-circadianclock2.jpg.

http://www.mc.uky.edu/ (n.d.), http://www.mc.uky.edu/pharmacology/instruction/pha824mp/pha824

http://www.medterms.com/ (n.d.), http://www.medterms.com/script/main/art.asp?articlekey=5236.

http://www.systemsbiology.org/ (n.d.), http://www.systemsbiology.org/.

Hughes, A. T., Fahey, B., Cutler, D. J., Coogan, A. N. & Piggins, H. D. (2004), 'Aberrant gating of photic input to the suprachiasmatic circadian pacemaker of mice lacking the vpac2 receptor', *The Journal of Neuroscience* **24**(14), 3522–3526.
URL: *http://www.jneurosci.org/content/24/14/3522.abstract*

Itri, J. & Colwell, C. S. (2003*a*), 'Regulation of inhibitory synaptic transmission by vasoactive intestinal peptide (vip) in the mouse suprachiasmatic nucleus', *Journal of Neurophysiology* **90**(3), 1589–1597.

Itri, J. & Colwell, C. S. (2003*b*), 'Regulation of inhibitory synaptic transmission by vasoactive intestinal peptide (vip) in the mouse suprachiasmatic nucleus', *Journal of Neurophysiology* **90**(3), 1589–1597.

Johnson, R., Moore, R. & Morin, L. (1988), 'Loss of entrainment and anatomical plasticity after lesions of the hamster retinohypothalamic tract', *Brain Research* **460**(2), 297 – 313.

URL: *http://www.sciencedirect.com/science/article/B6SYR-4840JMF-BV/2/107fce462ec5ba12276c20bebc04243e*

Kamaishi, H., Endoh, T. & Suzuki, T. (2004), 'Multiple signal pathways coupling vip and pacap receptors to calcium channels in hamster submandibular ganglion neurons', *Autonomic Neuroscience* **111**(1), 15 – 26.
URL: *http://www.sciencedirect.com/science/article/B6VT5-4BV52NH-1/2/daf125f2e8c117910ff9e52d30de9aac*

Kirschner, M. (2005), 'The meaning of systems biology', *Cell* **121**(4), 503–504.

Knutson, K., Spiegel, K., Penev, P. & Van Cauter, E. (2007), 'The metabolic consequences of sleep deprivation.', *Sleep medicine reviews* **11**(3), 163–178.

Latta, F. & Van Cauter, E. (2003), *Handbook of Psychology*, John Wiley & Sons Inc., chapter Sleep and Biological Clocks.

Lauffenburger, D. & Linderman, J. (1996), *Receptors: Models for Binding, Trafficking, and Signaling*, Oxford University Press.

Leloup, J.-C. & Goldbeter, A. (2003), 'Toward a detailed computational model for the mammalian circadian clock', *Proceedings of the National Academy of Sciences of the United States of America* **100**(12), 7051–7056.

Maywood, E., O'Neill, J., Chesham, J. & Hastings, M. (2007), 'Minireview: The circadian clockwork of the suprachiasmatic nuclei–analysis of a cellular oscillator that drives endocrine rhythms.', *Endocrinology* **148**(12), 5624–5634.

Maywood, E. S., Reddy, A. B., Wong, G. K. Y., O'Neill, J. S., O'Brien, J. A., McMahon, D. G., Harmar, A. J., Okamura, H. & Hastings, M. H. (2006), 'Synchronization and maintenance of timekeeping in suprachiasmatic circadian clock cells by neuropeptidergic signaling', *Current Biology* **16**(6), 599–605.

URL: *http://www.sciencedirect.com/science/article/B6VRT-4JHMFT0-Y/2/7c77fbdcf0115107789a17a9f622c9ff*

Mirsky, H., Liu, A., Welsh, D., Kay, S. & Doyle III, F. (2009), 'A model of the cell-autonomous mammalian circadian clock.', *Proceedings of the National Academy of Sciences of the United States of America* **106**(27), 11107–11112.

Mirsky, H. P. (2010), Modeling and Analysis of the Mammalian Circadian Clock, PhD thesis, University of California Santa Barbara.

Murray, J. (2007), *Mathematical Biology: I. An Introduction (Interdisciplinary Applied Mathematics) (Pt. 1)*, 3rd edn, Springer.

Ospeck, M. C., Coffey, B. & Freeman, D. (2009), 'Light-dark cycle memory in the mammalian suprachiasmatic nucleus', *Biophysical journal* **97**(6), 1513–1524.
URL: *http://linkinghub.elsevier.com/retrieve/pii/S000634950901114X*

Piggins, H. & Cutler, D. (2003), 'The roles of vasoactive intestinal polypeptide in the mammalian circadian clock', *J Endocrinol* **177**(1), 7–15.
URL: *http://joe.endocrinology-journals.org/cgi/content/abstract/177/1/7*

Polynikis, A., Hogan, S. & di Bernardo, M. (2009), 'Comparing different ode modelling approaches for gene regulatory networks', *Journal of Theoretical Biology* .

Rusnak, M., E. Tóth, Z., House, S. B. & Gainer, H. (2007), 'Depolarization and neurotransmitter regulation of vasopressin gene expression in the rat suprachiasmatic nucleus in vitro', *The Journal of Neuroscience* **27**(1), 141–151.

Shinohara, K., Funabashi, T. & Kimura, F. (1999), 'Temporal profiles of vasoactive intestinal polypeptide precursor mrna and its receptor mrna in

the rat suprachiasmatic nucleus', *Molecular Brain Research* **63**(2), 262–267. **URL:** *http://www.sciencedirect.com/science/article/B6T07-3VH80K8-8/2/e699bdf1260f1593d27ff4b6d9f65471*

Shinohara, K., Tominaga, K., Isobe, Y. & Inouye, S. (1993), 'Photic regulation of peptides located in the ventrolateral subdivision of the suprachiasmatic nucleus of the rat: daily variations of vasoactive intestinal polypeptide, gastrin-releasing peptide, and neuropeptide y', *The Journal of Neuroscience* **13**(2), 793–800.

Susaki, E., Stelling, J. & Ueda, H. (2010), 'Challenges in synthetically designing mammalian circadian clocks', *Current Opinion in Biotechnology* .

Takahashi, M. & Arito, H. (2000), 'Maintenance of alertness and performance by a brief nap after lunch under prior sleep deficit', *Sleep* **23**(6), 813–819.

Thomas, M., Sing, H., Belenky, G., Holcomb, H., Mayberg, H., Dannals, R., Wagner, H., Thorne, D., Popp, K., Rowland, L., Welsh, A., Balwinski, S. & Redmond, D. (2000), 'Neural basis of alertness and cognitive performance impairments during sleepiness. i. effects of 24 h of sleep deprivation on waking human regional brain activity.', *Journal of sleep research* **9**(4), 335–352.

To, T., Henson, M., Herzog, E. & Doyle III, F. (2007), 'A molecular model for intercellular synchronization in the mammalian circadian clock', *Biophysical Journal* **92**(11), 3792–3803.

Ukai-Tadenuma, M., Yamada, R., Xu, H., Ripperger, J., Liu, A. & Ueda, H. (2011), 'Delay in feedback repression by cryptochrome 1 is required for circadian clock function', *Cell* .

Vosko, A. M., Schroeder, A., Loh, D. H. & Colwell, C. S. (2007), 'Vasoactive intestinal peptide and the mammalian circadian system', *General and Comparative Endocrinology* **152**(2-3), 165–175.

URL: *http://www.sciencedirect.com/science/article/B6WG0-4NTRT2C-1/2/f3205df3b8004d0c1161a59bf98bf3df*

Webb, A., Angelo, N., Huettner, J. & Herzog, E. (2009), 'Intrinsic, nondeterministic circadian rhythm generation in identified mammalian neurons.', *Proceedings of the National Academy of Sciences of the United States of America* **106**(38), 16493–16498.

Weber, F. (2009), 'Remodeling the clock: coactivators and signal transduction in the circadian clockworks', *Naturwissenschaften* .

Appendix A

Appendix

CODICE SingleCellAutoModel.m

```
function dydt = SingleCellAutoModel(t,y,B) %#ok<INUSL>
% State Variables ————————————————————————————————————
MP1 = y(1,:);
MP2 = y(2,:);
MC1 = y(3,:);
MC2 = y(4,:);
MREV = y(5,:);
MCLK = y(6,:);
MBM1 = y(7,:);
MROR = y(8,:);
P1 = y(9,:);
P2 = y(10,:);
C1 = y(11,:);
C2 = y(12,:);
REV = y(13,:);
CLK = y(14,:);
BM1 = y(15,:);
ROR = y(16,:);
P1C1 = y(17,:);
```

```
P2C1 = y(18,:);
P1C2 = y(19,:);
P2C2 = y(20,:);
CLKBM1 = y(21,:);

% Parameters
vs0P1 = B(1);
vs1P1 = B(2);
vs0P2 = B(3);
vs1P2 = B(4);
vs0C1 = B(5);
vs1C1 = B(6);
vs2C1 = B(7);
vs0C2 = B(8);
vs1C2 = B(9);
vs2C2 = B(10);
vs1REV = B(11);
vs0CLK = B(12);
vs1CLK = B(13);
vs0BM1 = B(14);
vs1BM1 = B(15);
vs0ROR = B(16);
vs1ROR = B(17);
vs2ROR = B(18);

na1_P1 = B(19);
ni1_P1 = B(20);
ni2_P1 = B(21);
ni3_P1 = B(22);
ni4_P1 = B(23);
na1_P2 = B(24);
ni1_P2 = B(25);
ni2_P2 = B(26);
ni3_P2 = B(27);
```

```
ni4_P2 = B(28);
na1_C1 = B(29);
na2_C1 = B(30);
ni1_C1 = B(31);
ni2_C1 = B(32);
ni3_C1 = B(33);
ni4_C1 = B(34);
na1_C2 = B(35);
na2_C2 = B(36);
ni1_C2 = B(37);
ni2_C2 = B(38);
ni3_C2 = B(39);
ni4_C2 = B(40);
na1_REV = B(41);
ni1_REV = B(42);
ni2_REV = B(43);
ni3_REV = B(44);
ni4_REV = B(45);
na1_CLK = B(46);
ni1_CLK = B(47);
na1_BM1 = B(48);
ni1_BM1 = B(49);
na1_ROR = B(50);
na2_ROR = B(51);
ni1_ROR = B(52);
ni2_ROR = B(53);
ni3_ROR = B(54);
ni4_ROR = B(55);

KA1P1 = B(56);
KI1P1 = B(57);
KI2P1 = B(58);
KI3P1 = B(59);
KI4P1 = B(60);
```

```
KA1P2 = B(61);
KI1P2 = B(62);
KI2P2 = B(63);
KI3P2 = B(64);
KI4P2 = B(65);
KA1C1 = B(66);
KA2C1 = B(67);
KI1C1 = B(68);
KI2C1 = B(69);
KI3C1 = B(70);
KI4C1 = B(71);
KA1C2 = B(72);
KA2C2 = B(73);
KI1C2 = B(74);
KI2C2 = B(75);
KI3C2 = B(76);
KI4C2 = B(77);
KA1REV = B(78);
KI1REV = B(79);
KI2REV = B(80);
KI3REV = B(81);
KI4REV = B(82);
KA1CLK = B(83);
KI1CLK = B(84);
KA1BM1 = B(85);
KI1BM1 = B(86);
KA1ROR = B(87);
KA2ROR = B(88);
KI1ROR = B(89);
KI2ROR = B(90);
KI3ROR = B(91);
KI4ROR = B(92);

kdmP1 = B(93);
```

```
kdmP2 = B(94);
kdmC1 = B(95);
kdmC2 = B(96);
kdmREV = B(97);
kdmCLK = B(98);
kdmBM1 = B(99);
kdmROR = B(100);

tlP1  = B(101);
tlP2  = B(102);
tlC1  = B(103);
tlC2  = B(104);
tlREV = B(105);
tlCLK = B(106);
tlBM1 = B(107);
tlROR = B(108);

upP1  = B(109);
upP2  = B(110);
upC1 = B(111);
upC2 = B(112);
upREV = B(113);
upCLK = B(114);
upBM1 = B(115);
upROR = B(116);

arP1C1 = B(117);
arP1C2 = B(118);
arP2C1 = B(119);
arP2C2 = B(120);
arCLKBM1 = B(121);

drP1C1 = B(122);
drP1C2 = B(123);
```

```
drP2C1 = B(124);
drP2C2 = B(125);
drCLKBM1 = B(126);

ni5_C1 = B(127);
ni5_C2 = B(128);
ni5_ROR = B(129);
KI5C1 = B(130);
KI5C2 = B(131);
KI5ROR = B(132);

% ODEs
dydt(1,:) = (vs0P1+vs1P1.*(CLKBM1.^na1_P1)./(KA1P1.^na1_P1+...
    CLKBM1.^na1_P1)).*(KI1P1.^ni1_P1)./(KI1P1.^ni1_P1+P1C1.^ni1_P1).*...
    (KI2P1.^ni2_P1)./(KI2P1.^ni2_P1+P1C2.^ni2_P1).*(KI3P1.^ni3_P1)./...
    (KI3P1.^ni3_P1+P2C1.^ni3_P1).*(KI4P1.^ni4_P1)./(KI4P1.^ni4_P1+...
P2C2.^ni4_P1)-kdmP1.*MP1;
dydt(2,:) = (vs0P2+vs1P2.*(CLKBM1.^na1_P2)./(KA1P2.^na1_P2+...
    CLKBM1.^na1_P2)).*(KI1P2.^ni1_P2)./(KI1P2.^ni1_P2+P1C1.^ni1_P2).*...
    (KI2P2.^ni2_P2)./(KI2P2.^ni2_P2+P1C2.^ni2_P2).*(KI3P2.^ni3_P2)./...
    (KI3P2.^ni3_P2+P2C1.^ni3_P2).*(KI4P2.^ni4_P2)./(KI4P2.^ni4_P2+...
    P2C2.^ni4_P2)-kdmP2.*MP2;
dydt(3,:) = (vs0C1+vs1C1.*(CLKBM1.^na1_C1)./(KA1C1.^na1_C1+...
    CLKBM1.^na1_C1)+vs2C1.*(ROR.^na2_C1)./(KA2C1.^na2_C1+ROR.^na2_C1)).*...
(KI1C1.^ni1_C1)./(KI1C1.^ni1_C1+P1C1.^ni1_C1).*(KI2C1.^ni2_C1)./...
(KI2C1.^ni2_C1+P1C2.^ni2_C1).*(KI3C1.^ni3_C1)./(KI3C1.^ni3_C1+...
P2C1.^ni3_C1).*(KI4C1.^ni4_C1)./(KI4C1.^ni4_C1+P2C2.^ni4_C1).*...
(KI5C1.^ni5_C1)./(KI5C1.^ni5_C1+REV.^ni5_C1)-kdmC1.*MC1;
dydt(4,:) = (vs0C2+vs1C2.*(CLKBM1.^na1_C2)./(KA1C2.^na1_C2+...
    CLKBM1.^na1_C2)+vs2C2.*(ROR.^na2_C2)./(KA2C2.^na2_C2+...
    ROR.^na2_C2)).*(KI1C2.^ni1_C2)./(KI1C2.^ni1_C2+P1C1.^ni1_C2).*...
    (KI2C2.^ni2_C2)./(KI2C2.^ni2_C2+P1C2.^ni2_C2).*(KI3C2.^ni3_C2)./...
    (KI3C2.^ni3_C2+P2C1.^ni3_C2).*(KI4C2.^ni4_C2)./(KI4C2.^ni4_C2+...
    P2C2.^ni4_C2).*(KI5C2.^ni5_C2)./(KI5C2.^ni5_C2+REV.^ni5_C2)-kdmC2.*MC2;
```

```
dydt(5,:) = vs1REV.*(CLKBM1.^na1_REV)./(KA1REV.^na1_REV+...
    CLKBM1.^na1_REV).*(KI1REV.^ni1_REV)./(KI1REV.^ni1_REV+...
    P1C1.^ni1_REV).*(KI2REV.^ni2_REV)./(KI2REV.^ni2_REV+P1C2.^ni2_REV).*...
    (KI3REV.^ni3_REV)./(KI3REV.^ni3_REV+P2C1.^ni3_REV).*...
    (KI4REV.^ni4_REV)./(KI4REV.^ni4_REV+P2C2.^ni4_REV)-kdmREV.*MREV;
dydt(6,:) = (vs0CLK+vs1CLK.*(ROR.^na1_CLK)./(KA1CLK.^na1_CLK+...
    ROR.^na1_CLK)).*(KI1CLK.^ni1_CLK)./(KI1CLK.^ni1_CLK+REV.^ni1_CLK)-...
    kdmCLK.*MCLK;
dydt(7,:) = (vs0BM1+vs1BM1.*(ROR.^na1_BM1)./(KA1BM1.^na1_BM1+...
    ROR.^na1_BM1)).*(KI1BM1.^ni1_BM1)./(KI1BM1.^ni1_BM1+REV.^ni1_BM1)-...
    kdmBM1.*MBM1;
dydt(8,:) = (vs0ROR+vs1ROR.*(CLKBM1.^na1_ROR)./(KA1ROR.^na1_ROR+...
    CLKBM1.^na1_ROR)+vs2ROR.*(ROR.^na2_ROR)./(KA2ROR.^na2_ROR+...
    ROR.^na2_ROR)).*(KI1ROR.^ni1_ROR)./(KI1ROR.^ni1_ROR+P1C1.^ni1_ROR).*...
    (KI2ROR.^ni2_ROR)./(KI2ROR.^ni2_ROR+P1C2.^ni2_ROR).*...
    (KI3ROR.^ni3_ROR)./(KI3ROR.^ni3_ROR+P2C1.^ni3_ROR).*...
    (KI4ROR.^ni4_ROR)./(KI4ROR.^ni4_ROR+P2C2.^ni4_ROR).*...
    (KI5ROR.^ni5_ROR)./(KI5ROR.^ni5_ROR+REV.^ni5_ROR)-kdmROR.*MROR;

dydt(9,:) = tlP1.*MP1 - upP1.*P1 - arP1C1.*P1.*C1 - arP1C2.*P1.*C2 + ...
    drP1C1.*P1C1 + drP1C2.*P1C2;
dydt(10,:) = tlP2.*MP2 - upP2.*P2 - arP2C1.*P2.*C1 - arP2C2.*P2.*C2 + ...
    drP2C1.*P2C1 + drP2C2.*P2C2;
dydt(11,:) = tlC1.*MC1 - upC1.*C1 - arP1C1.*P1.*C1 - arP2C1.*P2.*C1 + ...
    drP1C1.*P1C1 + drP2C1.*P2C1;
dydt(12,:) = tlC2.*MC2 - upC2.*C2 - arP1C2.*P1.*C2 - arP2C2.*P2.*C2 + ...
    drP1C2.*P1C2 + drP2C2.*P2C2;
dydt(13,:) = tlREV.*MREV - upREV.*REV;
dydt(14,:) = tlCLK.*MCLK - upCLK.*CLK - arCLKBM1.*CLK.*BM1 + drCLKBM1.*...
    CLKBM1;
dydt(15,:) = tlBM1.*MBM1 - upBM1.*BM1 - arCLKBM1.*CLK.*BM1 + drCLKBM1.*...
    CLKBM1;
dydt(16,:) = tlROR.*MROR - upROR.*ROR;
```

```
dydt(17,:) = arP1C1.*P1.*C1 - drP1C1.*P1C1;
dydt(18,:) = arP2C1.*P2.*C1 - drP2C1.*P2C1;
dydt(19,:) = arP1C2.*P1.*C2 - drP1C2.*P1C2;
dydt(20,:) = arP2C2.*P2.*C2 - drP2C2.*P2C2;
dydt(21,:) = arCLKBM1.*CLK.*BM1 - drCLKBM1.*CLKBM1;
end
```

CODICE VPACcoupled_mm.m

```
function dydt = VPACcoupled_mm(t,y,ncells,B,newParams,varargin)
%VIP release controllato non piu da per2 mrna ma da totale p2 protein
dydt = zeros(size(y));
if (nargin>5)
   cputimeinit = varargin{1};
   assert(etime(clock, cputimeinit) < 60*10);
end
cellnos = 1:ncells;
% State Variables
MP1(cellnos,:) = y((cellnos-1)*23+1,:);
MP2(cellnos,:) = y((cellnos-1)*23+2,:);
MC1(cellnos,:) = y((cellnos-1)*23+3,:);
MC2(cellnos,:) = y((cellnos-1)*23+4,:);
MREV(cellnos,:) = y((cellnos-1)*23+5,:);
MCLK(cellnos,:) = y((cellnos-1)*23+6,:);
MBM1(cellnos,:) = y((cellnos-1)*23+7,:);
MROR(cellnos,:) = y((cellnos-1)*23+8,:);
P1(cellnos,:) = y((cellnos-1)*23+9,:);
P2(cellnos,:) = y((cellnos-1)*23+10,:);
C1(cellnos,:) = y((cellnos-1)*23+11,:);
C2(cellnos,:) = y((cellnos-1)*23+12,:);
REV(cellnos,:) = y((cellnos-1)*23+13,:);
CLK(cellnos,:) = y((cellnos-1)*23+14,:);
BM1(cellnos,:) = y((cellnos-1)*23+15,:);
ROR(cellnos,:) = y((cellnos-1)*23+16,:);
```

```
P1C1(cellnos,:) = y((cellnos-1)*23+17,:);
P2C1(cellnos,:) = y((cellnos-1)*23+18,:);
P1C2(cellnos,:) = y((cellnos-1)*23+19,:);
P2C2(cellnos,:) = y((cellnos-1)*23+20,:);
CLKBM1(cellnos,:) = y((cellnos-1)*23+21,:);
CB(cellnos,:) = y((cellnos-1)*23+22,:);
VIP_VPAC2(cellnos,:)=y((cellnos-1)*23+23,:);


% Parameters
vs0P1 = B(1);
vs1P1 = B(2);
vs0P2 = B(3);
vs1P2 = B(4);
vs0C1 = B(5);
vs1C1 = B(6);
vs2C1 = B(7);
vs0C2 = B(8);
vs1C2 = B(9);
vs2C2 = B(10);
vs1REV = B(11);
vs0CLK = B(12);
vs1CLK = B(13);
vs0BM1 = B(14);
vs1BM1 = B(15);
vs0ROR = B(16);
vs1ROR = B(17);
vs2ROR = B(18);

na1_P1 = B(19);
ni1_P1 = B(20);
ni2_P1 = B(21);
ni3_P1 = B(22);
ni4_P1 = B(23);
```

```
na1_P2 = B(24);
ni1_P2 = B(25);
ni2_P2 = B(26);
ni3_P2 = B(27);
ni4_P2 = B(28);
na1_C1 = B(29);
na2_C1 = B(30);
ni1_C1 = B(31);
ni2_C1 = B(32);
ni3_C1 = B(33);
ni4_C1 = B(34);
na1_C2 = B(35);
na2_C2 = B(36);
ni1_C2 = B(37);
ni2_C2 = B(38);
ni3_C2 = B(39);
ni4_C2 = B(40);
na1_REV = B(41);
ni1_REV = B(42);
ni2_REV = B(43);
ni3_REV = B(44);
ni4_REV = B(45);
na1_CLK = B(46);
ni1_CLK = B(47);
na1_BM1 = B(48);
ni1_BM1 = B(49);
na1_ROR = B(50);
na2_ROR = B(51);
ni1_ROR = B(52);
ni2_ROR = B(53);
ni3_ROR = B(54);
ni4_ROR = B(55);

KA1P1 = B(56);
```

```
KI1P1 = B(57);
KI2P1 = B(58);
KI3P1 = B(59);
KI4P1 = B(60);
KA1P2 = B(61);
KI1P2 = B(62);
KI2P2 = B(63);
KI3P2 = B(64);
KI4P2 = B(65);
KA1C1 = B(66);
KA2C1 = B(67);
KI1C1 = B(68);
KI2C1 = B(69);
KI3C1 = B(70);
KI4C1 = B(71);
KA1C2 = B(72);
KA2C2 = B(73);
KI1C2 = B(74);
KI2C2 = B(75);
KI3C2 = B(76);
KI4C2 = B(77);
KA1REV = B(78);
KI1REV = B(79);
KI2REV = B(80);
KI3REV = B(81);
KI4REV = B(82);
KA1CLK = B(83);
KI1CLK = B(84);
KA1BM1 = B(85);
KI1BM1 = B(86);
KA1ROR = B(87);
KA2ROR = B(88);
KI1ROR = B(89);
KI2ROR = B(90);
```

```
KI3ROR = B(91);
KI4ROR = B(92);

kdmP1 = B(93);
kdmP2 = B(94);
kdmC1 = B(95);
kdmC2 = B(96);
kdmREV = B(97);
kdmCLK = B(98);
kdmBM1 = B(99);
kdmROR = B(100);

tlP1  = B(101);
tlP2  = B(102);
tlC1  = B(103);
tlC2  = B(104);
tlREV = B(105);
tlCLK = B(106);
tlBM1 = B(107);
tlROR = B(108);

upP1  = B(109);
upP2  = B(110);
upC1 = B(111);
upC2 = B(112);
upREV = B(113);
upCLK = B(114);
upBM1 = B(115);
upROR = B(116);

arP1C1 = B(117);
arP1C2 = B(118);
arP2C1 = B(119);
arP2C2 = B(120);
```

```
arCLKBM1 = B(121);

drP1C1 = B(122);
drP1C2 = B(123);
drP2C1 = B(124);
drP2C2 = B(125);
drCLKBM1 = B(126);

ni5_C1 = B(127);
ni5_C2 = B(128);
ni5_ROR = B(129);
KI5C1 = B(130);
KI5C2 = B(131);
KI5ROR = B(132);

k = newParams(1);
v0 = newParams(2);
v1 = newParams(3);
vP = newParams(4);
VMK = newParams(5);
Ka = newParams(6);
K_1 = newParams(7);
K_2 = newParams(8);
CBT = newParams(9);
KD = newParams(10);
a = newParams(11);
b = newParams(12);
vs2P1 = newParams(13);
vs2P2 = newParams(14);
KA2P1 = newParams(15);
KA2P2 = newParams(16);
na2_P1 = newParams(17);
na2_P2 = newParams(18);
na_CB = newParams(19);
```

```
KbVIP_VPAC2=newParams(20);%parametro aggiunto per non aver piu' VPAC2 costante
KVIP_VPAC2=newParams(21);
v0VPAC=newParams(22);
v1VPAC=newParams(23);
%totalP2=366.4617;

KfVIP_VPAC2=KbVIP_VPAC2/KD;

%r=extracellular VIP a=max rate of estracell VIP conc prod, b=Per mRNA conc at which V
%production is 1/2 its maximum
P2T(cellnos,:)=P2(cellnos,:)+P2C1(cellnos,:)+P2C2(cellnos,:);
VPAC2(cellnos,:)=v0VPAC+v1VPAC*P2T(cellnos,:)./(KVIP_VPAC2+P2T(cellnos,:));
r(cellnos,:) = a*(MP1(cellnos,:)+MP2(cellnos,:))./(b+MP1(cellnos,:)+MP2(cellnos,:));

%Spatial effects
%g=To rectified hypothesis:VIP available to cells(g(i)=VIP seen by cell i)
s = sqrt(ncells);
locmat = reshape(cellnos,s,s);
g = zeros(ncells,size(y,2));
contrib = zeros(ncells,1);
for i = 1:ncells
    [I,J] = find(locmat ~= i);%tutti gli indici meno del nodo in esame
    [currx,curry] = find(locmat==i);%indici nodo in esame
    distances = sqrt((I-currx).^2 + (J-curry).^2);

    indices = (J-1)*s + I;
    contrib(indices) = 1./distances;
    contrib(i) = 1;
    g = g + contrib/sum(contrib)*r(i,:);
end

CCa(cellnos,:) = (v0+v1*VIP_VPAC2(cellnos,:))/k;
vK(cellnos,:) = VMK*CCa(cellnos,:)./(Ka+CCa(cellnos,:));
```

```
P1upreg =  vs2P1*((CBT*CB(cellnos,:)).^na2_P1)./...
    (KA2P1^na2_P1 + (CBT*CB(cellnos,:)).^na2_P1);
P2upreg =  vs2P2*((CBT*CB(cellnos,:)).^na2_P2)./...
    (KA2P2^na2_P2+(CBT*CB(cellnos,:)).^na2_P2);

dydt((cellnos-1)*23+1,:)  = (vs0P1+vs1P1*(CLKBM1(cellnos,:).^na1_P1)./...
    (KA1P1^na1_P1+CLKBM1(cellnos,:).^na1_P1) +P1upreg).*(KI1P1^ni1_P1)./...
    (KI1P1^ni1_P1+P1C1(cellnos,:).^ni1_P1).*(KI2P1^ni2_P1)./...
    (KI2P1^ni2_P1+P1C2(cellnos,:).^ni2_P1)*(KI3P1^ni3_P1)./...
    (KI3P1^ni3_P1+P2C1(cellnos,:).^ni3_P1).*(KI4P1^ni4_P1)./...
    (KI4P1^ni4_P1+P2C2(cellnos,:).^ni4_P1) - kdmP1*MP1(cellnos,:);
dydt((cellnos-1)*23+2,:)  = (vs0P2+vs1P2*(CLKBM1(cellnos,:).^na1_P2)./...
    (KA1P2^na1_P2+CLKBM1(cellnos,:).^na1_P2) +P2upreg).*(KI1P2^ni1_P2)./...
    (KI1P2^ni1_P2 + P1C1(cellnos,:).^ni1_P2).*(KI2P2^ni2_P2)./...
    (KI2P2^ni2_P2+P1C2(cellnos,:).^ni2_P2)*(KI3P2^ni3_P2)./...
    (KI3P2^ni3_P2+P2C1(cellnos,:).^ni3_P2).*(KI4P2^ni4_P2)./...
    (KI4P2^ni4_P2+P2C2(cellnos,:).^ni4_P2) - kdmP2*MP2(cellnos,:);
dydt((cellnos-1)*23+3,:)  = (vs0C1+vs1C1*(CLKBM1(cellnos,:).^na1_C1)./...
    (KA1C1^na1_C1+CLKBM1(cellnos,:).^na1_C1) + vs2C1*...
    (ROR(cellnos,:).^na2_C1)./(KA2C1^na2_C1+ROR(cellnos,:).^na2_C1))*...
    (KI1C1^ni1_C1)./(KI1C1^ni1_C1+P1C1(cellnos,:).^ni1_C1)*...
    (KI2C1^ni2_C1)./(KI2C1^ni2_C1+P1C2(cellnos,:).^ni2_C1)*...
    (KI3C1^ni3_C1)./(KI3C1^ni3_C1+P2C1(cellnos,:).^ni3_C1)*...
    (KI4C1^ni4_C1)./(KI4C1^ni4_C1+P2C2(cellnos,:).^ni4_C1)*...
    (KI5C1^ni5_C1)./(KI5C1^ni5_C1+REV(cellnos,:).^ni5_C1) -...
    kdmC1*MC1(cellnos,:);
dydt((cellnos-1)*23+4,:)  = (vs0C2+vs1C2*(CLKBM1(cellnos,:).^na1_C2)./...
    (KA1C2^na1_C2+CLKBM1(cellnos,:).^na1_C2) + vs2C2*...
    (ROR(cellnos,:).^na2_C2)./(KA2C2^na2_C2+ROR(cellnos,:).^na2_C2))*...
    (KI1C2^ni1_C2)./(KI1C2^ni1_C2+P1C1(cellnos,:).^ni1_C2)*...
    (KI2C2^ni2_C2)./(KI2C2^ni2_C2+P1C2(cellnos,:).^ni2_C2)*...
    (KI3C2^ni3_C2)./(KI3C2^ni3_C2+P2C1(cellnos,:).^ni3_C2)*...
    (KI4C2^ni4_C2)./(KI4C2^ni4_C2+P2C2(cellnos,:).^ni4_C2)*...
```

```
    (KI5C2^ni5_C2)./(KI5C2^ni5_C2+REV(cellnos,:).^ni5_C2) −...
    kdmC2*MC2(cellnos,:);
dydt((cellnos−1)*23+5,:)  = vs1REV*(CLKBM1(cellnos,:).^na1_REV)./...
    (KA1REV^na1_REV+CLKBM1(cellnos,:).^na1_REV)*(KI1REV^ni1_REV)./...
    (KI1REV^ni1_REV+P1C1(cellnos,:).^ni1_REV)*(KI2REV^ni2_REV)./...
    (KI2REV^ni2_REV+P1C2(cellnos,:).^ni2_REV)*(KI3REV^ni3_REV)./...
    (KI3REV^ni3_REV+P2C1(cellnos,:).^ni3_REV)*(KI4REV^ni4_REV)./...
    (KI4REV^ni4_REV+P2C2(cellnos,:).^ni4_REV)−kdmREV*MREV(cellnos,:);
dydt((cellnos−1)*23+6,:)  = (vs0CLK+vs1CLK*(ROR(cellnos,:).^na1_CLK)./...
    (KA1CLK^na1_CLK+ROR(cellnos,:).^na1_CLK))*(KI1CLK^ni1_CLK)./...
    (KI1CLK^ni1_CLK+REV(cellnos,:).^ni1_CLK)−kdmCLK*MCLK(cellnos,:);
dydt((cellnos−1)*23+7,:)  = (vs0BM1+vs1BM1*(ROR(cellnos,:).^na1_BM1)./...
    (KA1BM1^na1_BM1+ROR(cellnos,:).^na1_BM1))*(KI1BM1^ni1_BM1)./...
    (KI1BM1^ni1_BM1+REV(cellnos,:).^ni1_BM1)−kdmBM1*MBM1(cellnos,:);
dydt((cellnos−1)*23+8,:)  =(vs0ROR+vs1ROR*(CLKBM1(cellnos,:).^na1_ROR)./...
    (KA1ROR^na1_ROR+CLKBM1(cellnos,:).^na1_ROR) + vs2ROR*...
    (ROR(cellnos,:).^na2_ROR)./(KA2ROR^na2_ROR+ROR(cellnos,:).^na2_ROR))*...
    (KI1ROR^ni1_ROR)./(KI1ROR^ni1_ROR+P1C1(cellnos,:).^ni1_ROR)*...
    (KI2ROR^ni2_ROR)./(KI2ROR^ni2_ROR+P1C2(cellnos,:).^ni2_ROR)*...
    (KI3ROR^ni3_ROR)./(KI3ROR^ni3_ROR+P2C1(cellnos,:).^ni3_ROR).*...
    (KI4ROR^ni4_ROR)./(KI4ROR^ni4_ROR+P2C2(cellnos,:).^ni4_ROR).*...
    (KI5ROR^ni5_ROR)./(KI5ROR^ni5_ROR+REV(cellnos,:).^ni5_ROR) − ...
    kdmROR*MROR(cellnos,:);

dydt((cellnos−1)*23+9,:)  = tlP1*MP1(cellnos,:) − upP1*P1(cellnos,:)...
    − arP1C1*P1(cellnos,:).*C1(cellnos,:) − arP1C2*P1(cellnos,:).*...
    C2(cellnos,:) + drP1C1*P1C1(cellnos,:) + drP1C2*P1C2(cellnos,:);
dydt((cellnos−1)*23+10,:) = tlP2*MP2(cellnos,:) − upP2*P2(cellnos,:) − ...
    arP2C1*P2(cellnos,:).*C1(cellnos,:) − arP2C2*P2(cellnos,:).*...
    C2(cellnos,:) + drP2C1*P2C1(cellnos,:) + drP2C2*P2C2(cellnos,:);
dydt((cellnos−1)*23+11,:) = tlC1*MC1(cellnos,:) − upC1*C1(cellnos,:) − ...
    arP1C1*P1(cellnos,:).*C1(cellnos,:) − arP2C1*P2(cellnos,:).*...
    C1(cellnos,:) + drP1C1*P1C1(cellnos,:) + drP2C1*P2C1(cellnos,:);
dydt((cellnos−1)*23+12,:) = tlC2*MC2(cellnos,:) − upC2*C2(cellnos,:) − ...
```

```
    arP1C2*P1(cellnos,:).*C2(cellnos,:) - arP2C2*P2(cellnos,:).*...
    C2(cellnos,:) + drP1C2*P1C2(cellnos,:) + drP2C2*P2C2(cellnos,:);
dydt((cellnos-1)*23+13,:) = tlREV*MREV(cellnos,:) - upREV*REV(cellnos,:);
dydt((cellnos-1)*23+14,:) = tlCLK*MCLK(cellnos,:) - upCLK*...
    CLK(cellnos,:) - arCLKBM1*CLK(cellnos,:).*BM1(cellnos,:) +...
    drCLKBM1.*CLKBM1(cellnos,:);
dydt((cellnos-1)*23+15,:) = tlBM1*MBM1(cellnos,:) - upBM1*...
    BM1(cellnos,:) - arCLKBM1*CLK(cellnos,:).*BM1(cellnos,:) +...
    drCLKBM1.*CLKBM1(cellnos,:);
dydt((cellnos-1)*23+16,:) = tlROR*MROR(cellnos,:) - upROR*ROR(cellnos,:);

dydt((cellnos-1)*23+17,:) = arP1C1*P1(cellnos,:).*C1(cellnos,:) -...
    drP1C1*P1C1(cellnos,:);
dydt((cellnos-1)*23+18,:) = arP2C1*P2(cellnos,:).*C1(cellnos,:) -...
    drP2C1*P2C1(cellnos,:);
dydt((cellnos-1)*23+19,:) = arP1C2*P1(cellnos,:).*C2(cellnos,:) -...
    drP1C2*P1C2(cellnos,:);
dydt((cellnos-1)*23+20,:) = arP2C2*P2(cellnos,:).*C2(cellnos,:) -...
    drP2C2*P2C2(cellnos,:);
dydt((cellnos-1)*23+21,:) = arCLKBM1*CLK(cellnos,:).*BM1(cellnos,:) - ...
    drCLKBM1*CLKBM1(cellnos,:);

dydt((cellnos-1)*23+22,:) = (vP/CBT)*(vK(cellnos,:)./vP.*(1-...
    CB(cellnos,:)).^na_CB./(K_1^na_CB+(1-CB(cellnos,:)).^na_CB)-...
    CB(cellnos,:).^na_CB./(K_2^na_CB+CB(cellnos,:).^na_CB));
dydt((cellnos-1)*23+23,:)=KfVIP_VPAC2*VPAC2(cellnos,:).*g(cellnos,:)-...
    KbVIP_VPAC2*VIP_VPAC2(cellnos,:);
```

CODICE VPACmRNA.m

```
function dydt = VPACmRNA(t,y,ncells,B,newParams,varargin)
%VIP release controllato non piu da per2 mrna ma da totale p2 protein
dydt = zeros(size(y));
```

```
if (nargin>5)
   cputimeinit = varargin{1};
   assert(etime(clock, cputimeinit) < 60*10);
end
cellnos = 1:ncells;
% State Variables
MP1(cellnos,:) = y((cellnos-1)*24+1,:);
MP2(cellnos,:) = y((cellnos-1)*24+2,:);
MC1(cellnos,:) = y((cellnos-1)*24+3,:);
MC2(cellnos,:) = y((cellnos-1)*24+4,:);
MREV(cellnos,:) = y((cellnos-1)*24+5,:);
MCLK(cellnos,:) = y((cellnos-1)*24+6,:);
MBM1(cellnos,:) = y((cellnos-1)*24+7,:);
MROR(cellnos,:) = y((cellnos-1)*24+8,:);
P1(cellnos,:) = y((cellnos-1)*24+9,:);
P2(cellnos,:) = y((cellnos-1)*24+10,:);
C1(cellnos,:) = y((cellnos-1)*24+11,:);
C2(cellnos,:) = y((cellnos-1)*24+12,:);
REV(cellnos,:) = y((cellnos-1)*24+13,:);
CLK(cellnos,:) = y((cellnos-1)*24+14,:);
BM1(cellnos,:) = y((cellnos-1)*24+15,:);
ROR(cellnos,:) = y((cellnos-1)*24+16,:);
P1C1(cellnos,:) = y((cellnos-1)*24+17,:);
P2C1(cellnos,:) = y((cellnos-1)*24+18,:);
P1C2(cellnos,:) = y((cellnos-1)*24+19,:);
P2C2(cellnos,:) = y((cellnos-1)*24+20,:);
CLKBM1(cellnos,:) = y((cellnos-1)*24+21,:);
CB(cellnos,:) = y((cellnos-1)*24+22,:);
VIP_VPAC2(cellnos,:)=y((cellnos-1)*24+23,:);
VPAC2(cellnos,:)=y((cellnos-1)*24+24,:);


% Parameters
```

```
vs0P1 = B(1);
vs1P1 = B(2);
vs0P2 = B(3);
vs1P2 = B(4);
vs0C1 = B(5);
vs1C1 = B(6);
vs2C1 = B(7);
vs0C2 = B(8);
vs1C2 = B(9);
vs2C2 = B(10);
vs1REV = B(11);
vs0CLK = B(12);
vs1CLK = B(13);
vs0BM1 = B(14);
vs1BM1 = B(15);
vs0ROR = B(16);
vs1ROR = B(17);
vs2ROR = B(18);

na1_P1 = B(19);
ni1_P1 = B(20);
ni2_P1 = B(21);
ni3_P1 = B(22);
ni4_P1 = B(23);
na1_P2 = B(24);
ni1_P2 = B(25);
ni2_P2 = B(26);
ni3_P2 = B(27);
ni4_P2 = B(28);
na1_C1 = B(29);
na2_C1 = B(30);
ni1_C1 = B(31);
ni2_C1 = B(32);
ni3_C1 = B(33);
```

```
ni4_C1 = B(34);
na1_C2 = B(35);
na2_C2 = B(36);
ni1_C2 = B(37);
ni2_C2 = B(38);
ni3_C2 = B(39);
ni4_C2 = B(40);
na1_REV = B(41);
ni1_REV = B(42);
ni2_REV = B(43);
ni3_REV = B(44);
ni4_REV = B(45);
na1_CLK = B(46);
ni1_CLK = B(47);
na1_BM1 = B(48);
ni1_BM1 = B(49);
na1_ROR = B(50);
na2_ROR = B(51);
ni1_ROR = B(52);
ni2_ROR = B(53);
ni3_ROR = B(54);
ni4_ROR = B(55);

KA1P1 = B(56);
KI1P1 = B(57);
KI2P1 = B(58);
KI3P1 = B(59);
KI4P1 = B(60);
KA1P2 = B(61);
KI1P2 = B(62);
KI2P2 = B(63);
KI3P2 = B(64);
KI4P2 = B(65);
KA1C1 = B(66);
```

```
KA2C1 = B(67);
KI1C1 = B(68);
KI2C1 = B(69);
KI3C1 = B(70);
KI4C1 = B(71);
KA1C2 = B(72);
KA2C2 = B(73);
KI1C2 = B(74);
KI2C2 = B(75);
KI3C2 = B(76);
KI4C2 = B(77);
KA1REV = B(78);
KI1REV = B(79);
KI2REV = B(80);
KI3REV = B(81);
KI4REV = B(82);
KA1CLK = B(83);
KI1CLK = B(84);
KA1BM1 = B(85);
KI1BM1 = B(86);
KA1ROR = B(87);
KA2ROR = B(88);
KI1ROR = B(89);
KI2ROR = B(90);
KI3ROR = B(91);
KI4ROR = B(92);

kdmP1 = B(93);
kdmP2 = B(94);
kdmC1 = B(95);
kdmC2 = B(96);
kdmREV = B(97);
kdmCLK = B(98);
kdmBM1 = B(99);
```

```
kdmROR = B(100);

tlP1  = B(101);
tlP2  = B(102);
tlC1  = B(103);
tlC2  = B(104);
tlREV = B(105);
tlCLK = B(106);
tlBM1 = B(107);
tlROR = B(108);

upP1  = B(109);
upP2  = B(110);
upC1 = B(111);
upC2 = B(112);
upREV = B(113);
upCLK = B(114);
upBM1 = B(115);
upROR = B(116);

arP1C1 = B(117);
arP1C2 = B(118);
arP2C1 = B(119);
arP2C2 = B(120);
arCLKBM1 = B(121);

drP1C1 = B(122);
drP1C2 = B(123);
drP2C1 = B(124);
drP2C2 = B(125);
drCLKBM1 = B(126);

ni5_C1 = B(127);
ni5_C2 = B(128);
```

```
ni5_ROR = B(129);
KI5C1 = B(130);
KI5C2 = B(131);
KI5ROR = B(132);

k = newParams(1);
v0 = newParams(2);
v1 = newParams(3);
vP = newParams(4);
VMK = newParams(5);
Ka = newParams(6);
K_1 = newParams(7);
K_2 = newParams(8);
CBT = newParams(9);
KD = newParams(10);
a = newParams(11);
b = newParams(12);
vs2P1 = newParams(13);
vs2P2 = newParams(14);
KA2P1 = newParams(15);
KA2P2 = newParams(16);
na2_P1 = newParams(17);
na2_P2 = newParams(18);
na_CB = newParams(19);
KbVIP_VPAC2=newParams(20);%da qui in poi nuovi parametri aggiunti per ...
%non aver piu' VPAC2 costante
KMVPAC2=newParams(21);
v0MVPAC=newParams(22);
v1MVPAC=newParams(23);
tlVPAC2=newParams(24);%translation rate
degVPAC2T=newParams(25);%degradation rate
KintVIP_VPAC2=newParams(26);

%totalP2=366.4617;
```

```
KfVIP_VPAC2=KbVIP_VPAC2/KD;

%r=extracellular VIP a=max rate of estracell VIP conc prod,
%b=Per mRNA conc at which VIP production is 1/2 its maximum
MVPAC(cellnos,:)=v0MVPAC+v1MVPAC*MP2(cellnos,:)./...
    (KMVPAC2+MP2(cellnos,:));
r(cellnos,:) = a*(MP1(cellnos,:)+MP2(cellnos,:))./...
    (b+MP1(cellnos,:)+MP2(cellnos,:));

%Spatial effects
%g=To rectified hypothesis:VIP available to cells(g(i)=VIP seen by cell i)
s = sqrt(ncells);
locmat = reshape(cellnos,s,s);
g = zeros(ncells,size(y,2));
contrib = zeros(ncells,1);
for i = 1:ncells
    [I,J] = find(locmat ~= i);%tutti gli indici meno del nodo in esame
    [currx,curry] = find(locmat==i);%indici nodo in esame
    distances = sqrt((I-currx).^2 + (J-curry).^2);

    indices = (J-1)*s + I;
    contrib(indices) = 1./distances;
    contrib(i) = 1;
    g = g + contrib/sum(contrib)*r(i,:);
end

if (nargin == 7)
    pulse = varargin{2};
    if (t>=pulse(1) && t< (pulse(1) + pulse(2)))
        g(cellnos,:) = g(cellnos,:) + pulse(3);
    end
end
```

```
CCa(cellnos,:) = (v0+v1*VIP_VPAC2(cellnos,:))/k;
vK(cellnos,:) = VMK*CCa(cellnos,:)./(Ka+CCa(cellnos,:));


P1upreg =  vs2P1*((CBT*CB(cellnos,:)).^na2_P1)./...
    (KA2P1^na2_P1 + (CBT*CB(cellnos,:)).^na2_P1);
P2upreg =  vs2P2*((CBT*CB(cellnos,:)).^na2_P2)./...
    (KA2P2^na2_P2+(CBT*CB(cellnos,:)).^na2_P2);

dydt((cellnos-1)*24+1,:)  = (vs0P1+vs1P1*(CLKBM1(cellnos,:).^na1_P1)./...
    (KA1P1^na1_P1+CLKBM1(cellnos,:).^na1_P1) +P1upreg).*(KI1P1^ni1_P1)./...
    (KI1P1^ni1_P1+P1C1(cellnos,:).^ni1_P1).*(KI2P1^ni2_P1)./...
    (KI2P1^ni2_P1+P1C2(cellnos,:).^ni2_P1)...
    *(KI3P1^ni3_P1)./(KI3P1^ni3_P1+P2C1(cellnos,:).^ni3_P1).*...
    (KI4P1^ni4_P1)./(KI4P1^ni4_P1+P2C2(cellnos,:).^ni4_P1) -...
    kdmP1*MP1(cellnos,:);
dydt((cellnos-1)*24+2,:)  = (vs0P2+vs1P2*(CLKBM1(cellnos,:).^na1_P2)./...
    (KA1P2^na1_P2+CLKBM1(cellnos,:).^na1_P2) +P2upreg).*(KI1P2^ni1_P2)./...
    (KI1P2^ni1_P2 + P1C1(cellnos,:).^ni1_P2).*(KI2P2^ni2_P2)./...
    (KI2P2^ni2_P2+P1C2(cellnos,:).^ni2_P2)*(KI3P2^ni3_P2)./...
    (KI3P2^ni3_P2+P2C1(cellnos,:).^ni3_P2).*(KI4P2^ni4_P2)./...
    (KI4P2^ni4_P2+P2C2(cellnos,:).^ni4_P2)- kdmP2*MP2(cellnos,:);
dydt((cellnos-1)*24+3,:)  = (vs0C1+vs1C1*(CLKBM1(cellnos,:).^na1_C1)./...
    (KA1C1^na1_C1+CLKBM1(cellnos,:).^na1_C1)...
    + vs2C1*(ROR(cellnos,:).^na2_C1)./(KA2C1^na2_C1+ROR(cellnos,:)...
    .^na2_C1))*(KI1C1^ni1_C1)./...
    (KI1C1^ni1_C1+P1C1(cellnos,:).^ni1_C1)*(KI2C1^ni2_C1)./...
    (KI2C1^ni2_C1+P1C2(cellnos,:).^ni2_C1)*(KI3C1^ni3_C1)./...
    (KI3C1^ni3_C1+P2C1(cellnos,:).^ni3_C1)*(KI4C1^ni4_C1)./...
    (KI4C1^ni4_C1+P2C2(cellnos,:).^ni4_C1)*(KI5C1^ni5_C1)./...
    (KI5C1^ni5_C1+REV(cellnos,:).^ni5_C1) ...
    - kdmC1*MC1(cellnos,:);
dydt((cellnos-1)*24+4,:)  = (vs0C2+vs1C2*(CLKBM1(cellnos,:).^na1_C2)./...
    (KA1C2^na1_C2+CLKBM1(cellnos,:).^na1_C2) +...
```

```
    vs2C2*(ROR(cellnos,:).^na2_C2)./(KA2C2^na2_C2+...
    ROR(cellnos,:).^na2_C2))*(KI1C2^ni1_C2)./...
    (KI1C2^ni1_C2+P1C1(cellnos,:).^ni1_C2)*(KI2C2^ni2_C2)./...
    (KI2C2^ni2_C2+P1C2(cellnos,:).^ni2_C2)*...
    (KI3C2^ni3_C2)./(KI3C2^ni3_C2+P2C1(cellnos,:).^ni3_C2)*...
    (KI4C2^ni4_C2)./(KI4C2^ni4_C2+P2C2(cellnos,:).^ni4_C2)*...
    (KI5C2^ni5_C2)./(KI5C2^ni5_C2+REV(cellnos,:).^ni5_C2) -...
    kdmC2*MC2(cellnos,:);
dydt((cellnos-1)*24+5,:)  = vs1REV*(CLKBM1(cellnos,:).^na1_REV)./...
    (KA1REV^na1_REV+CLKBM1(cellnos,:).^na1_REV)*...
    (KI1REV^ni1_REV)./(KI1REV^ni1_REV+P1C1(cellnos,:).^ni1_REV)*...
    (KI2REV^ni2_REV)./(KI2REV^ni2_REV+P1C2(cellnos,:).^ni2_REV)*...
    (KI3REV^ni3_REV)./(KI3REV^ni3_REV+P2C1(cellnos,:).^ni3_REV)*...
    (KI4REV^ni4_REV)./(KI4REV^ni4_REV+P2C2(cellnos,:).^ni4_REV)-...
    kdmREV*MREV(cellnos,:);
dydt((cellnos-1)*24+6,:)  = (vs0CLK+vs1CLK*(ROR(cellnos,:).^na1_CLK)./...
    (KA1CLK^na1_CLK+ROR(cellnos,:).^na1_CLK))*...
    (KI1CLK^ni1_CLK)./(KI1CLK^ni1_CLK+REV(cellnos,:).^ni1_CLK)-...
    kdmCLK*MCLK(cellnos,:);
dydt((cellnos-1)*24+7,:)  = (vs0BM1+vs1BM1*(ROR(cellnos,:).^na1_BM1)./...
    (KA1BM1^na1_BM1+ROR(cellnos,:).^na1_BM1))*...
    (KI1BM1^ni1_BM1)./(KI1BM1^ni1_BM1+REV(cellnos,:).^ni1_BM1)-...
    kdmBM1*MBM1(cellnos,:);
dydt((cellnos-1)*24+8,:)  =(vs0ROR+vs1ROR*(CLKBM1(cellnos,:).^na1_ROR)./...
    (KA1ROR^na1_ROR+CLKBM1(cellnos,:).^na1_ROR) + vs2ROR*...
    (ROR(cellnos,:).^na2_ROR)./(KA2ROR^na2_ROR+...
    ROR(cellnos,:).^na2_ROR))*(KI1ROR^ni1_ROR)./...
    (KI1ROR^ni1_ROR+P1C1(cellnos,:).^ni1_ROR)*...
    (KI2ROR^ni2_ROR)./(KI2ROR^ni2_ROR+P1C2(cellnos,:).^ni2_ROR)*...
    (KI3ROR^ni3_ROR)./(KI3ROR^ni3_ROR+P2C1(cellnos,:).^ni3_ROR).*...
    (KI4ROR^ni4_ROR)./(KI4ROR^ni4_ROR+P2C2(cellnos,:).^ni4_ROR).*...
    (KI5ROR^ni5_ROR)./(KI5ROR^ni5_ROR+REV(cellnos,:).^ni5_ROR) -...
    kdmROR*MROR(cellnos,:);
dydt((cellnos-1)*24+9,:)  = tlP1*MP1(cellnos,:) - upP1*P1(cellnos,:) -...
```

```
    arP1C1*P1(cellnos,:).*...
    C1(cellnos,:) - arP1C2*P1(cellnos,:).*C2(cellnos,:) + ...
    drP1C1*P1C1(cellnos,:) + drP1C2*P1C2(cellnos,:);
dydt((cellnos-1)*24+10,:) = tlP2*MP2(cellnos,:) - upP2*P2(cellnos,:) -...
    arP2C1*P2(cellnos,:).*...
    C1(cellnos,:) - arP2C2*P2(cellnos,:).*C2(cellnos,:) + ...
    drP2C1*P2C1(cellnos,:) + drP2C2*P2C2(cellnos,:);
dydt((cellnos-1)*24+11,:) = tlC1*MC1(cellnos,:) - upC1*C1(cellnos,:)...
    - arP1C1*P1(cellnos,:).*...
    C1(cellnos,:) - arP2C1*P2(cellnos,:).*C1(cellnos,:) + ...
    drP1C1*P1C1(cellnos,:) + drP2C1*P2C1(cellnos,:);
dydt((cellnos-1)*24+12,:) = tlC2*MC2(cellnos,:) - upC2*C2(cellnos,:) - ...
    arP1C2*P1(cellnos,:).*...
    C2(cellnos,:) - arP2C2*P2(cellnos,:).*C2(cellnos,:) + ...
    drP1C2*P1C2(cellnos,:) + drP2C2*P2C2(cellnos,:);
dydt((cellnos-1)*24+13,:) = tlREV*MREV(cellnos,:) - upREV*REV(cellnos,:);
dydt((cellnos-1)*24+14,:) = tlCLK*MCLK(cellnos,:) - upCLK*CLK(cellnos,:)...
    - arCLKBM1*CLK(cellnos,:).*...
    BM1(cellnos,:) + drCLKBM1.*CLKBM1(cellnos,:);
dydt((cellnos-1)*24+15,:) = tlBM1*MBM1(cellnos,:) - upBM1*BM1(cellnos,:)...
    - arCLKBM1*CLK(cellnos,:).*...
    BM1(cellnos,:) + drCLKBM1.*CLKBM1(cellnos,:);
dydt((cellnos-1)*24+16,:) = tlROR*MROR(cellnos,:) - upROR*ROR(cellnos,:);
dydt((cellnos-1)*24+17,:) = arP1C1*P1(cellnos,:).*C1(cellnos,:) -...
    drP1C1*P1C1(cellnos,:);
dydt((cellnos-1)*24+18,:) = arP2C1*P2(cellnos,:).*C1(cellnos,:) -...
    drP2C1*P2C1(cellnos,:);
dydt((cellnos-1)*24+19,:) = arP1C2*P1(cellnos,:).*C2(cellnos,:) - ...
    drP1C2*P1C2(cellnos,:);
dydt((cellnos-1)*24+20,:) = arP2C2*P2(cellnos,:).*C2(cellnos,:) - ...
    drP2C2*P2C2(cellnos,:);
dydt((cellnos-1)*24+21,:) = arCLKBM1*CLK(cellnos,:).*BM1(cellnos,:) - ...
    drCLKBM1*CLKBM1(cellnos,:);
dydt((cellnos-1)*24+22,:) = (vP/CBT)*(vK(cellnos,:)./vP.*...
```

```
    (1-CB(cellnos,:)).^na_CB./(K_1^na_CB+(1-CB(cellnos,:)).^na_CB)-...
    CB(cellnos,:).^na_CB./(K_2^na_CB+CB(cellnos,:).^na_CB));
dydt((cellnos-1)*24+23,:) = KfVIP_VPAC2*VPAC2(cellnos,:).*g(cellnos,:)...
    -KbVIP_VPAC2*VIP_VPAC2(cellnos,:)-...
    KintVIP_VPAC2*VIP_VPAC2(cellnos,:);
dydt((cellnos-1)*24+24,:) = tlVPAC2.*MVPAC(cellnos,:)-...
    degVPAC2T.*VPAC2(cellnos,:)+KbVIP_VPAC2*VIP_VPAC2(cellnos,:)-...
    KfVIP_VPAC2*VPAC2(cellnos,:).*g(cellnos,:);
```

CODICE Cla_cost_fun_peak.m

```
function cost = Cla_cost_fun_peak(ParameterSet,varargin)
%CLA_COST_FUN_SIMPLE Summary of this function goes here
%   Detailed explanation goes here


% Change parameter range
load parameterSet.mat parameterSet;

ps=[16.6941;0.6520;3.1082;1.8032;10.8895;2.3009;0.2434;0.2434;1.8450;...
    2.1229;45.6755;5.2815;98.1526;38.7838;4.0549;0.7079;2.6408;2.8029;...
    1.8987;1.5000;5.0000;2.0000; 1.5000];

lb=ps/5;
ub=ps*5;
newParameters = lb + (exp(ParameterSet')-1)/(exp(1)-1).*(ub-lb);
%newParameters = ParameterSet';

IC1 = ones(21,1);

options = odeset('RelTol',1e-4,'Vectorized','on');
[t,y] = ode15s(@SingleCellAutoModel,0:0.1:500,IC1,options,parameterSet);
Y = y(size(y,1)-2048+1:size(y,1),10);
Y = Y - mean(Y);
```

```
[Pxx,fxx] = periodogram(Y,[],[],5);
[m, mind] = max(Pxx);
period = 1/fxx(mind);

y = y(end-720:end,:);

ncells=16;
IC2 = zeros(1,ncells*23);


for i = 1:ncells
    for j = 1:21
        IC2((i-1)*23+j) = y(1+round((i-1)*(period*10)/ncells),j);
    end
    IC2((i-1)*23+22) =0.5;
    IC2((i-1)*23+23) =0;
end
IC2 = reshape(IC2,23,ncells);
IC2(:,randperm(ncells)) = IC2;
IC2 = reshape(IC2,ncells*23,1);
clear t
clear y


events = @(t,y,varargin) events_peak(t,y,VPACcoupled_mm(t,y,...
    ncells,parameterSet,newParameters));
options = odeset('RelTol',1e-6,'AbsTol',1e-8,'Vectorized','on',...
    'MaxStep',0.1*period);


T = [0,1500];
%T = linspace(0,1500,4096);
flag = 0;
cputimeinit = clock;
```

```
try
    [t,y] = ode15s(@VPACcoupled_mm,T,IC2,options,ncells,parameterSet,...
        newParameters,cputimeinit);
catch ME
   flag = 1; %se ci mette piu' di 5 ore si ferma
end



if(~flag)
    t0 = t(end);
    y0 = y(end,:)';
    clear t y;
    options = odeset('RelTol',1e-7,'AbsTol',1e-9,'Vectorized','on',...
        'MaxStep',0.1*period,'Events',events);


    cputimeinit = clock;
    try
        [t,y,te,ye,ie] = ode15s(@VPACcoupled_mm,[t0,t0+60],y0,options,...
            ncells,parameterSet,newParameters,cputimeinit);
    catch ME
        flag=1;
    end
    coupledperiod = diff(te(find(ie==1,2,'first')));
    if (isempty(coupledperiod) || coupledperiod<15)
        cost = 50000;
  else
      phi=zeros(ncells,1);
      empty=0;
     for i=1:ncells
         if(isempty(te(find(ie==i,1,'first'))))
             empty=empty+1;
```

```
        end
    end
    if (empty==0)
    for i=1:ncells
        phi(i) = 2*pi*(te(find(ie==i,1,'first'))-te(find(ie==1,1,...
            'first')))/coupledperiod;
    end

   SI = abs(sum(exp(1i*phi)))/ncells;
   cost = 50*(1-SI);
    else
        cost=5000;
    end
end
  else cost = 100000;
end

return
```

CODICE events_peak.m

```
function [value,isterminal,direction] = events_peak(t,y,deriv)
ncells = round(size(y,1)/23);
value = deriv((0:ncells-1)*23+10,:) + deriv((0:ncells-1)*23+18,:) +...
    deriv((0:ncells-1)*23+20,:);
isterminal = 0*ones(ncells,1);
direction = -1*ones(ncells,1);
end
```

Acknowledgements - Ringraziamenti

I am really grateful to my advisor, Prof. Francis J. Doyle III, and to my mentor, Dr. Bharath Ananthasubramaniam for giving me the great opportunity to be a part of their group and for stimulating my work. I have been very lucky to have interacted with such wondeful graduate students and post doctoral fellows, especially for sharing the office with Pegy, Bharath and Yongquiang.

Questa tesi mi ha accompagnata nellarco dei sei mesi in cui ho vissuto lesperienza piú forte di tutta la mia vita. Ringrazio innanzitutto la professoressa Barbara Di Camillo, il professor Francis J. Doyle III e Bharath Ananthasubramaniam per avermi dato fiducia e avermi regalato la grande possibilitá di lavorare a questo progetto. Ringrazio Celia per aver corretto il mio inglese.

Questa tesi mi ha portato lontano da tutto e tutti, sola, ad affrontare ogni cosa, per dimostrare agli altri ma soprattutto a me stessa che sarei stata in grado di superare anche la prova piú grande di tutte: diventare grande e arrangiarmi da sola. Ho imparato quanto sia bello sentirsi a casa, avere una famiglia ad aspettarti la sera. Ho imparato quanto unamicizia possa cambiare lottica di ogni cosa e come basti davvero poco per passare dalle stelle al piú fondo buio quando ci si sente soli.

Ringrazio i miei genitori, per aver spesso sacrificato in silenzio tanti loro

desideri senza che me ne accorgessi, pur di dare a me il piú possibile, mettendoci tutto il loro amore. Per aver sempre creduto nelle mie capacitá e avermi aiutata ad accettare i miei errori e le mie delusioni quando, spinta dalla mia ostinazione a perseguire i miei obiettivi, talvolta non riuscivo ad accontentarmi di dovermi fermare davanti ai miei limiti. Grazie per aver sopportato i miei sfoghi nei momenti di crisi e quando credevo che non ce lavrei mai fatta. Sono sicura che senza di voi non sarei mai arrivata fin qui oggi. Grazie per non avermi mai detto quanto difficile fosse per voi lasciarmi partire. Grazie per aver accettato e sostenuto anche questa mia scelta seppur contro i vostri desideri, come per tutte le altre decisioni importanti che mi son trovata a prendere fino ad oggi, senza provare mai ad influenzarmi e lasciandomi la piena libertá e responsabilitá di scelta. Mi avete aiutata a crescere.

Grazie a Gianluca, per farmi sentire unamica, oltre che una sorella, ogni volta che vuoi un mio consiglio, che mi chiedi di riparare ai tuoi disastri e che mi confidi i tuoi segreti. E stato bello avere una stanza singola per un po', ma solo per non doversi svegliare ogni mattina con le tue insopportabili sveglie, in fondo mi piace sapere che sei sempre vicino a me, in ogni senso.

Ringrazio Tomaso, per esser il mio punto fisso e la mia certezza, per esser lunica persona in grado di farmi star tranquilla e ricordarmi sempre quali sono le cose a cui merita dar del peso nella vita. Grazie per non esserti fatto spaventare dai sei mesi di lontananza. Saresti stato forse lunico in grado di farmi cambiare idea riguardo la mia partenza.

Grazie a tutte le mie amiche Erica, Teresa, Fanny ed Elisa per tutti i bei momenti assieme, per esser sempre state presenti e per avermi fatto sentire il vostro affetto anche dallaltra parte del mondo. Un ringraziamento speciale a Marta con cui ho condiviso piú che con chiunque altro ogni mio momento piú felice e per esser sempre pronta a darmi un saggio consiglio nel momento del

bisogno. Grazie ad Eleonora, perché per me sei e sarai sempre la solita Leo che mi rubava le Kinder Pinguí dal frigo, con cui posso litigare e continuare a volerti bene come prima. Grazie a Filippo, per esser il mio secondo Giadrossi preferito. Grazie a Sprits, per aver attraversato tre stati per portare un po' di casa a Santa Barbara e per avermi aiutato nel rendere piú presentabile questa tesi. Grazie a Ozz, per dare a tutti prova di grande carattere. Grazie a Giorgia, Ale, Bon, Gab e Lollo per i sabato sera assieme.

Un grazie enorme a tutti i miei compagni di universitá, per tutto il tempo, tutte le fatiche e tutte le risate assieme. Pensare di venire a trovare voi a Padova ogni mattina quando mi svegliavo alle 6,45 per andare a lezione, rendeva tutto piú piacevole e sopportabile. Un grazie speciale a Stefano, per aver sempre potuto contare sulla tua presenza, come compagno di viaggio ma soprattutto come amico. Grazie ad Andrea per le chiacchere assieme, per i tuoi suggerimenti su libri e film e perché non vederti in treno la mattina mi faceva sempre sperare che la tua pigrizia potesse significare un passaggio in macchina per il ritorno. Grazie a Doni, per avermi dimostrato quanta forza abbiano il sorriso e lumiltá. Grazie a Deborah per tutto laffetto sincero che mi dimostri sempre. Grazie a Chiara Z. per esser il mio buon esempio da seguire. Grazie a Francesca liscia e Isabella per i pettegolezzi e i risotti in compagnia. Grazie ad Alice per le corse assieme verso la stazione e le lunghe mail. Grazie a Francesca riccia per aver portato sempre un po' di spensieratezza e serenitá in aula. Grazie a Pippo, Chiara G., Chiara B., Mauro e Biru, Onelia e quanti non nomino solo per non dilungarmi troppo. Spero davvero che la nostra amicizia non finisca con la nostra laurea.